Universidad Nacional Autónoma de México

PROGRAMA DE MAESTRÍA Y DOCTORADO EN INGENIERÍA

CONTROL DE DESPLAZAMIENTO Y FUERZA DE UN PISTÓN NEUMÁTICO DIFERENCIAL

(DISPLACEMENT AND FORCE CONTROL OF A DIFFERENTIAL PNEUMATIC ACTUATOR)

T E S I S

QUE PARA OBTAR POR EL GRADO DE

DOCTOR EN INGENIERÍA

INGENIERÍA ELECTRICA - CONTROL

Presenta:

JENS WEIST

Tutor:

Dr. MARCO ANTONIO ARTEAGA PÉREZ

MÉXICO, D.F.
2011

Jurado asignado

Presidente:	Dr. Luis Agustín Alvarez Icaza Longoría
Secretario:	Dr. Gerardo René Espinosa Pérez
Vocal:	Dr. Marco Antonio Arteaga Pérez
$1^{er.}$ Suplente:	Dr. Rafael Martínez Guerra
$2^{do.}$ Suplente:	Dr. Paul Rolando Maya Ortiz

Lugar donde se realizó la tesis:
Ciudad de México, D.F., México

TUTOR DE TESIS:
Dr. Marco Antonio Arteaga Pérez

FIRMA

Acknowledgements

This work is based on research supported by the **CONACYT** under grant **58112** and by **DGAPA–UNAM** under grant **IN105408**.

Also, the author and his tutor would like to express their gratitude to *Festo* for kindly donating many components of the experimental test best.

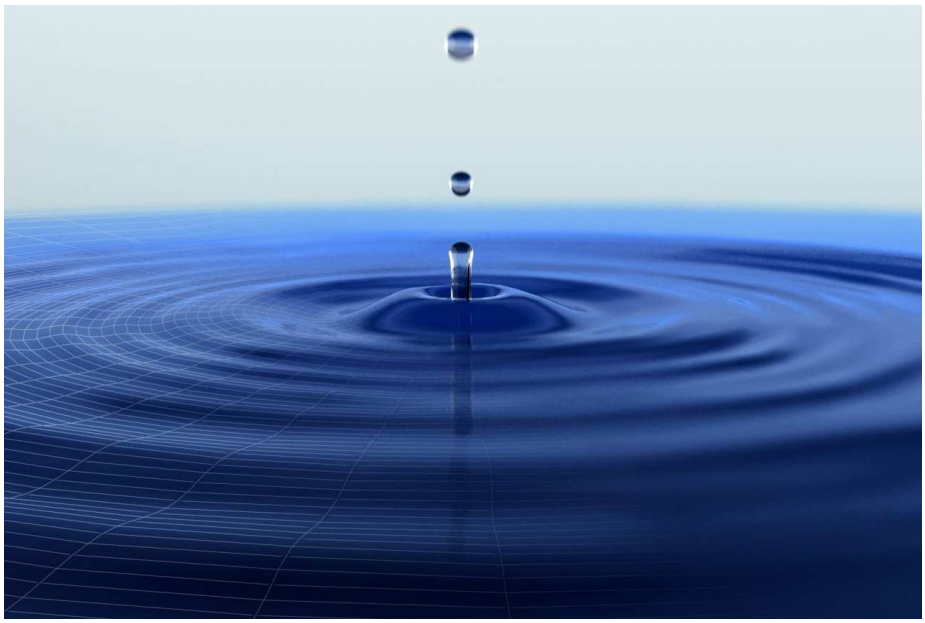

What we know is a drop,
what we don't know,
an ocean.

- Isaac Newton -

Personal acknowledgments

Le agradezco mucho a mi tutor Dr. Marco Antonio Arteaga Pérez por guiarme en este trabajo, por su paciencia y sobre todo por sus valiosos inspiraciónes.

Tambien les agradezco a Dr. Luis Agustín Alvarez Icaza Longoría, Dr. Gerardo René Espinosa Pérez, Dr. Rafael Martínez Guerra y Dr. Paul Rolando Maya Ortiz por formar el jurado de esta tesis. Gracias por sus numerosos comentarios.

Gracias a mis compañeros y amigos Carlo, Irvin, Juan, Juvenal y Maximilian por tantas discussiones y por incorporarme a sus vidas y la cultura mexicana.

Gracias a mi "hermano mexicano" Daniel y su familia por ser un gran amigo y por hacer inolvidable mi estancia en México.

Gracias a TODOS que no pude mencionar aqui en esta pagina personalmente. Con su amistad, su apollo y compania forman parte de cuatro maravillosos años en su pais.

Ich danke natrlich auch allen anderen Freunden und Bekannten, die mir im Rahmen dieser Dissertation auf Ihre Art beigestanden haben und mich in den Jahren im Ausland nicht vergessen haben.

Die Familie ist gerade im Rahmen eines Auslandsaufenthaltes zwar nicht direkt in das fachliche Geschehen eingebunden, dafür aber umso mehr im daheim gebliebenen Alltag mit allen Aufgaben und Hürden. Einen herzlichen Dank an meine Eltern Rosemarie und Jürgen, Ihr habt mit Euren Ratschlgen, für mich erledigte Bürokratengänge und sporadischen Finanzspritzen auch mageblich zum Gelingen dieser Arbeit beigetragen. Auch meinem Bruder Marc möchte ich für seinen Beitrag zum Ganzen danken. Herzlichen Dank für die fachlichen Diskussionen, die Einblicke in die reelle industrielle Anwendungswelt und auch für Deinen zahlreichen Organisationseinsatz.

Zu guter Letzt der persönlichen Danksagungen, möchte ich meiner lieben Frau Ana Lilia für Deine Unterstützung in allen Lagen und Gemütszuständen während der Anfertigung dieser Arbeit recht herzlich danken. Du warst letztendlich nicht nur der Stein des Anstoßes sondern auch eine der wichtigen treibenden Kräfte.

Un humano
Un hombre
Un alumno
Un maestro
Un colega
Un amigo

†

Jorge Lenin Ruiz Mejía

1978 - 2009

Contents

Abstract (English)

Simple PID control algorithms, based on the dynamic model are the most common for a high degree of tasks in the industry. Pneumatic systems are highly nonlinear systems, so that a control law based on the dynamic model will reach a maximum performance rather poor, caused by unmodeled uncertainties. In fact, the dynamic model can reach up to a 7-th order dynamic model or even more, considering *e. g.* only 2 orders of the piston, 2 orders for the valve, 1 order for the connection-tubes and 2 orders for friction models. This simple sum shows that it could be an interesting task to reflect the real nature considering all physical phenomenons of this nonlinear system and keep it in a still online computable order. May be nowadays, apart the before mentioned fact, it is technically feasible to compute control based on high order models, but for the main applications in the industry it is financially definitely not feasible.
In this work, some properties of the dynamic model of pneumatic actuators are analyzed and rewritten in the form as a cascade structure. Further a nonlinear PID is adapted for the control of force and displacement of the piston, based on the rewritten structure of the system. Later the proposed control law is implemented in a experimental test bed and it's performance is compared with other algorithms which do not require the dynamic model for implementation neither. Finally some conclusions are given.

Abstract (Spanish)

Algoritmos de control como PIDs sencillos o basados en el modelo dinámico son los mas communes en aplicaciones en la industria. Los sistemas neumáticos son, altamente no lineales y este hecho no es deseado en el diseño de controladores. Se puede ver facilmente que tarde o temprano un algoritmo de control basado en un modelo dinámico llegará a su máximo rendimiento posible, causado por las incertidumbres no modeladas. Se puede obtener un modelo de 7.$^{\text{mo}}$ orden o todavía mas, considerando solo por ejemplo 2 ordenes del piston, 2 ordenes de la válvula, 1 orden de la tubería y 2 ordenes de un modelo de fricción. Esa súma muestra que puede ser una tarea interesante modelar un sistema neumático, considerando todos los fenómenos físicos reales y dejarlo todavía de tal orden que se puede ejecutar en línea. Esto es importante porque la implementación de leyes de control complejas no es una práctica industrial. Esa es una de las principales razones de proponer una adaptación de un controlador PID no lineal.

Esta tesis muestra la adaptación de un controlador propuesto, asi como una breve introduccion, el desarollo de un modelo común de un sistema neumatico así como una forma del modelo matematico en cascada que será la base para la ley de control propuesta, la comparación experimental del controlador propuesto con dos controladores usados en la industria, un PID simple y un controlador de modos deslizantes de primer orden, un análisis de observabilidad y finalmente la conclusión.

Abstract (German)

Einfache PID's oder solche auf dynamischen Modellen basierende Regelungsalgorithmen sind die am Häufigsten in der Industrie eingesetzten. Auf Grund der Physik sind pneumatische Systeme stark nichtlinear, was gleichzeitig einen nicht gewollten Umstand darstellt. So ist es recht anschaulich, dass früher oder später eine auf dem mathematischen Modell beruhende Regelung an seine Grenzen stöt, bedingt durch nicht im Modell berücksichtigte Unsicherheiten. Recht schnell kann man zu einem Modell 7. Ordnung oder gar noch höher gelangen, sofern man zum Beispiel nur folgenden Rahmen der Einzelmodelle annimmt: 2. Ordnung vom Zylinder, 2. Ordnung vom Ventil, 1. Ordnung von den Anschlussleitungen und 2. Ordnung von Reibungsmodellen. Diese einfache Summe zeigt auf, dass es eine interessante Aufgabe darstellen kann die wirkliche Natur eines solches Systemes mit all seinen Phänomenen mathematisch zu erfassen und gleichzeitig auch noch datenverarbeitungstechnisch handhabbar zu bekommen. In der heutigen Zeit stünde die Technik schon zur Verfgung dies auch dies ableisten zu knnen, nur sind diese Lösungen in der Industrie in der Regel finanziell bisher noch untragbar. Dies ist auch einer der Gründe einen neuen angepassten Regelalgorithmus vorzuschlagen, welcher den Kern dieser Dissertation darstellt. Diese Arbeit beinhaltet eine kurze Einfhrung, die Anpassung eines vorgeschlagenen nichtlinearen PID, die Entwicklung eines Standardmodelles fr pneumatische Systeme, sowie dessen Aufteilung in zwei Einzelsysteme, einen Vergleich mit 2 anderen in der Industrie sehr gebruchlichen Regelalgorithmen, einem einfachen PID und einem Sliding Mode Regelalgorithmus 1. Ordnung, eine Beobachtbarkeitsanalyse und den Abschluss.

Chapter 1

Introduction

The wish to use the power stored in air or compressed air is older than two millenniums. The first time mentioned in the history was about 0 BC by the Greek Heron of Alexandria. He used compressed air to open and close temple doors, as mentioned in Beater (2007), and he wrote the first related paper named $\pi\upsilon\varepsilon\nu\mu\alpha\tau o$ (pneumato). The desire to use air as a power transmitting medium is still actual. The main advantage of pneumatic systems lies on their cleanness, low prices, excellent weight to force ratio and easy assembling. Industrial applications for this kind of devices are wide, for instance, in special environments as food productions, where clean environments are needed or in oil industry with flammable conditions. Therefore, it is important to design controllers for pneumatic systems capable to reach the same performance level as for electric or hydraulic actuators.
Displacement and force tracking of the piston are the main control goals for differential pneumatic devices. In both cases it is necessary to regulate the mass flow entering into the two chambers of the system. The mass flows, entering and leaving, cause alterations of the chamber pressures which generates variation of the forces affecting on both sides of the piston which produces movements, force application or even its standstill. So we can conclude that this process consists of various phenomenons of the areas fluid mechanics, thermodynamics and mechanics.
Depending on the actuator, it may be controlled by many kinds of valves, like simple ON/OFF arrangements or proportional devices. These last ones are the most common in control applications, generate mass flows which depend on the control input voltage or current e.g. a 5/3-valve, which means that it has 5 connections and 3 positions. The 3 positions of the spool inside the valve are: maximum 1, neutral in the middle position and maximum 2. As both chambers of the piston are connected to the same valve this means that, when the spool is in one of the maximum positions the mass flow is positive, entering, in one chamber and negative, leaving, in the opposite one.
Although in industry usually simple PID's controllers are employed, in recent years more approaches have been under research. In Ning and Bone (2002) and

Ning and Bone (2005) PVA–Controllers (proportional plus velocity plus acceleration control) and advanced PID's are proposed, while Göttert and Neumann (1999) and Göttert and Neumann (2007) employ exact linearization. This particular technique has the disadvantage of being model dependent, which tends to decrease performance because the model is usually not accurate. Flatness based control is developed in the work by Sawodny and Hildebrandt (2002). Another widely used technique is sliding mode theory. It has the advantage of being very robust while the system model is normally not employed. Some examples are given by Richer and Hurmuzlu (2000) and Shen *et al.* (2006). Other approaches are cascade control as shown by Perondi (2002), Sobczyk and Perondi (2006) and Guenther *et al.* (2006), model reference adaptive control (MRAC) as given in Zhu (2006), and neural networks as developed by Kothapalli and Hassan (2007).
As can be appreciated, in general the control algorithms may requiere model information (feedback linealization) or none at all (neural networks), and a natural question is which option is better. The drawback of model based control lies in getting an accurate mathematical description of the system. In the case of differential pneumatic pistons a good model could reach up to 5–th order (two states from the piston, two from the valve, one from the connection-tube) and may be even more complex if dynamic friction effects are considered. Furthermore, this kind of techniques may not be suitable for industrial implementation, because of high necessary investments or lack of computing power in PLC's or intelligent valve terminals.

Thus, model free control or algorithms with few system information should be considered as a better alternative, as long as its implementation is not complex and the resulting performance is acceptable. Thus in this thesis an adaptation of the robot control law given in Arteaga-Pérez *et al.* (2006) is used out for pneumatic systems and compared with two well–known algorithms available in the literature which where tested on a differential pneumatic piston test bed. If there are few works on control of pneumatic actuators, the research on observer design is still more scarce. Not even a handful of papers can be found about this topic. In Wu *et al.* (2003) an observability analysis is done, but only for the most simple case, by considering the displacement of the piston, y, is given. Some possible cases of available states of the system are deduced and some analysis is done too. Bigras (2002) developed an nonlinear observer for pressure estimation and Gulati (2005) and Pandian (2002) use an observer to estimate the pressures, which are the simplest states to measure.

As there are only a few works are published based on the cascade structure of the system with the force difference of the chambers as the control entrance, but it does not exists a research about model free control based an a cascade structure, this forms our problem to resolve and our motivation at the same time. The main contribution of this work is the model free design of an control law based on a cascade structure of the pneumatic system and further it's implementation in a experimental test bed and a comparison with two other model free control laws. Cause of the lack of a complete analysis of observability, the in this work shown analysis can be understood as a part the contribution too.

This thesis is structured as follows:

- Chapter 2: Shows the dynamic model for a differential piston
- Chapter 3: Two common and frequently used control laws are given, and a original one is designed
- Chapter 5: Includes experimental results of the implemented control laws of the previous chapter
- Chapter 4: An observability analysis of the pneumatic system is carried out
- Chapter 6: Conclusions and a short list about the national and international contributions of this work are given
- Appendix A: Information about the experimental test bed and model validation is presented
- Appendix B: Includes theorem proofs

Chapter 2

Dynamic model of pneumatic pistons

Figure 2.1 depicts the general structure of a differential pneumatic piston, where L [m] is the maximal piston displacement, y [m] is the piston displacement and $\dot{y}$ [m/s] is the corresponding velocity. For $i = 1, 2$, L_i [m] is the width of the dead zone of chamber i, d [m] is the piston diameter, A_i [m^2] is the cross section area of piston chamber i, V_i [m^3] is the volume in chamber i, V_{i0} [m^3] is the dead volume of chamber i including tubes, $\mathrm{d_v}$ [m] is the piston rod diameter, w [m] is the piston width, p_i [Pa] is the pressure of chamber i. Finally, F [N] is the applied force.

The model development for this kind of pneumatic system can be found in many works, *e. g.* Göttert and Neumann (1999), Sobczyk and Perondi (2006), Beater (2007), Kothapalli and Hassan (2007). To review the development and refresh some physical effects this, chapter shows at first the background of the dynamic model, based on Newton's second law and the first law of thermodynamics for adiabatic processes. As a matter of fact, two subsystems can be distinguished: a mechanical part and a pneumatic component. In the following sections, their dynamic models and its interconnection is explained.

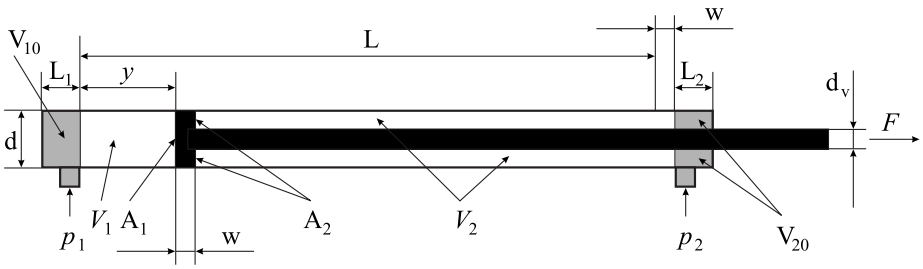

Figure 2.1: Differential pneumatic piston

2.1 Mechanical component dynamics

The main base to describe the mechanical part of the piston dynamics is Newton's second law (Böge, 1999). Since we can consider the mass of the system constant regarding the time, it's possible to use the following simple form:

$$F = \mathrm{M}a \tag{2.1}$$
$$F = \mathrm{M}\ddot{y} \tag{2.2}$$

with

$$F = \mathrm{A}p, \tag{2.3}$$

what brings us to

$$\ddot{y} = \frac{\mathrm{A}}{\mathrm{M}}p, \tag{2.4}$$

where

$$\begin{aligned} \mathrm{M} &: \text{system mass in movement [kg]} \\ a = \ddot{y} &: \text{acceleration } \left[\frac{\mathrm{m}}{\mathrm{s}^2}\right] \\ \mathrm{A} &: \text{area } \left[\mathrm{m}^2\right] \\ p &: \text{pressure } \left([\mathrm{Pa}] = \left[\frac{\mathrm{N}}{\mathrm{m}^2}\right]\right) \end{aligned}$$

In the case of a pneumatic differential piston there are forces on both sides, where the lowest pressure is given by the atmospheric pressure. To complete the model a term for viscose friction has been added, knowing that the real friction is much more complex that this term. As the model will not be used for the control law design this term is sufficient, alternatively a friction model like e.g. LuGre is recommended. So, based on equation (2.4) we get

$$F = \mathrm{M}\ddot{y} = \underbrace{\mathrm{A}_1(p_1 - \mathrm{p_{atm}})}_{F_1} - \underbrace{\mathrm{A}_2(p_2 - \mathrm{p_{atm}})}_{F_2} - \underbrace{F_\mathrm{v}\dot{y}}_{F_\mathrm{v}} \tag{2.5}$$

or

$$\ddot{y} = \frac{\mathrm{A}_1}{\mathrm{M}}p_1 - \frac{\mathrm{A}_2}{\mathrm{M}}p_2 - \frac{\mathrm{A}_1 - \mathrm{A}_2}{\mathrm{M}}\mathrm{p_{atm}} - \frac{F_\mathrm{v}}{\mathrm{M}}\dot{y} \tag{2.6}$$

where

p_{atm} : atmospheric pressure [Pa] = 101325[Pa] (DIN 1343, 1990)
F_1 : force generated in chamber 1 [N]
F_2 : force generated in chamber 2 [N]
F_v : viscose friction coefficient $\left[\frac{Ns}{m}\right]$
$v = \dot{y}$: velocity $\left[\frac{m}{s}\right]$
$a = \ddot{y}$: acceleration $\left[\frac{m}{s^2}\right]$

To calculate the pressures p_1 and p_2 some fundamental laws of thermodynamics are used and it is supposed that the internal process is adiabatic (without changes of the fluid-temperature), as investigated in Kagawa *et al.* (2002), so that we have an isothermal process. Additionally the principles of constant mass and the law of ideal gases are applied to obtain (Böge, 1999)

$$pV = mR_iT \tag{2.7}$$

with

p : pressure $\left([Pa] = \left[\frac{N}{m^2}\right]\right)$
V : volume $[m^3]$
m : mass of the gas [kg]
R_i : universal constant ideal gases $\left[\frac{J}{kgK}\right]$ (1[J] = 1[Nm]),
$R_i = 287\left[\frac{J}{kgK}\right]$ for air (at T = 273.15[K])
T : temperature [K].

Considering two particular cases: a) the Boyle-Mariotte law (Böge, 1999), which represents the behavior of a gas at a pressure change from an initial pressure p_i to a final pressure p_f with constant temperature T, we get

$$pV = \text{const} \tag{2.8}$$

$$\frac{p_i}{p_f} = \frac{V_f^{\gamma}}{V_i^{\gamma}} \tag{2.9}$$

$$\gamma = \frac{C_p}{C_v} \tag{2.10}$$

where (Böge, 1999)

p_i : initial pressure $\left([\mathrm{Pa}] = \left[\frac{\mathrm{N}}{\mathrm{m}^2}\right]\right)$

p_f : final pressure $\left(\mathrm{Pa} = \left[\frac{\mathrm{N}}{\mathrm{m}^2}\right]\right)$

V_i : initial volume $[\mathrm{m}^3]$

V_f : final volume $[\mathrm{m}^3]$

γ : coefficient of adiabatic dilatation

$\gamma = 1.4$ for air (at T = 273.15[K])

$\mathrm{C_p}$: calorific capacity at constant pressure $\left[\frac{\mathrm{J}}{\mathrm{kgK}}\right]$

$\mathrm{C_p} = 1005\left[\frac{\mathrm{J}}{\mathrm{kgK}}\right]$ for air (at T = 273.15[K])

$\mathrm{C_v}$: calorific capacity at constant volume $\left[\frac{\mathrm{J}}{\mathrm{kgK}}\right]$

$\mathrm{C_v} = 716\left[\frac{\mathrm{J}}{\mathrm{kgK}}\right]$ for air (at T = 273.15[K])

b) by the law of Gay-Lussac, which represents the behavior of a gas when the temperature changes from an initial value T_i to a final value T_f at a constant pressure p, (Böge, 1999)

$$\frac{V}{T} = \text{const} \tag{2.11}$$

$$\frac{V_\mathrm{i}}{V_\mathrm{f}} = \frac{T_\mathrm{i}^\gamma}{T_\mathrm{f}^\gamma} \tag{2.12}$$

with

T_i : initial temperature [K]

T_f : final temperature [K]

One can then describe the relation between internal and added energies by

$$U = H_1 - H_2 \tag{2.13}$$

U : internal energy, ($\mathrm{V_U}$=const)

H_1 : enthalpy added to the system

H_2 : enthalpy of the system (in form of work)

where

$$U = m\mathrm{C_v}T \tag{2.14}$$

$$H_1 = m\mathrm{C_p}\mathrm{T} \tag{2.15}$$

$$H_2 = m\mathrm{C_p}\mathrm{T} \tag{2.16}$$

Now, based on the factorized equation (2.7), we get

$$m = \frac{pV}{\mathrm{R_i}T} \tag{2.17}$$

and by factorizing (2.10) to the form

$$\mathrm{C_v} = \frac{\mathrm{C_p}}{\gamma} \tag{2.18}$$

one can rewrite

$$U = \frac{p\mathrm{V_U}\mathrm{C_v}T}{\mathrm{R_i}T} = \frac{\mathrm{C_p}p\mathrm{V_U}}{\gamma\mathrm{R_i}} \tag{2.19}$$

$$H_2 = \frac{p_{\mathrm{H2}}V\mathrm{C_p}T}{\mathrm{R_i}T} = \frac{\mathrm{C_p}p_{\mathrm{H2}}V}{\mathrm{R_i}} \tag{2.20}$$

where

V_{U} = constant volume based on the fact, that internal energy do not produces volume changing (see U from equation (2.13))

p_{H2} = constant pressure, based on the law of Gay-Lussac (see particular case b).

Rewriting equation (2.13) by combining previous relations one gets

$$\frac{\mathrm{C_p}p\mathrm{V_U}}{\gamma\mathrm{R_i}} = m\mathrm{C_p}\mathrm{T} - \frac{\mathrm{C_p}\mathrm{p_{H2}}V}{\mathrm{R_i}} \tag{2.21}$$

Factorizing the pressure

$$p = \frac{\gamma m\mathrm{R_i}\mathrm{T}}{\mathrm{V_U}} - \frac{\gamma\mathrm{p_{H2}}V}{\mathrm{V_U}} = \frac{\gamma}{\mathrm{V_U}}(m\mathrm{R_i}\mathrm{T} - \mathrm{p_{H2}}V) \tag{2.22}$$

and by differentiating

$$\dot{p} = \frac{\gamma}{\mathrm{V_U}}(\dot{m}\mathrm{R_i}\mathrm{T} - \mathrm{p_{H2}}\dot{V}) \tag{2.23}$$

Now, rewriting equation (2.23) for the specific system with $V = \mathrm{V_{10}} + V_1$ and $V = \mathrm{V_{20}} + V_2$, (where $V_1 = \mathrm{A_1}y$ and $V_2 = \mathrm{A_2}(\mathrm{L} - y)$) results

$$\dot{p_1} = \frac{\gamma}{\mathrm{V_{10}} + \mathrm{A_1}y}(\dot{m}_1\mathrm{R_i}T - p_1\dot{y}\mathrm{A_1}) \tag{2.24}$$

$$\dot{p_2} = \frac{\gamma}{\mathrm{V_{20}} + \mathrm{A_2}(\mathrm{L} - y)}(\dot{m}_2\mathrm{R_i}T - p_2\dot{y}\mathrm{A_2}) \tag{2.25}$$

with

$$\begin{aligned}
\dot{p_1} &: \text{pressure dynamics of chamber 1} \left[\frac{\text{Pa}}{\text{s}}\right] \\
\dot{m_1} &: \text{mass flow of chamber 1} \left[\frac{\text{kg}}{\text{s}}\right] \\
\dot{p_2} &: \text{pressure dynamics of chamber 2} \left[\frac{\text{Pa}}{\text{s}}\right] \\
\dot{m_2} &: \text{mass flow of chamber 2} \left[\frac{\text{kg}}{\text{s}}\right]
\end{aligned}$$

2.2 Pneumatic component dynamics

Equations (2.24) and (2.25) depend on the mass flows $\dot{m}_1$ and $\dot{m}_2$, which are parameters of the pneumatic system component and can be described, based on Göttert and Neumann (1999), as a special form of pneumatic resistance with a conductance C;

$$\dot{m} = C\rho\sqrt{\frac{\text{T}_0}{T}}p_\text{u}\psi \tag{2.26}$$

$$\psi = \psi\left(\frac{p_\text{d}}{p_\text{u}}, \text{b}\right) = \begin{cases} \sqrt{1-\left(\frac{\left(\frac{p_\text{d}}{p_\text{u}}-\text{b}\right)}{1-\text{b}}\right)^2} & , \frac{p_\text{d}}{p_\text{u}} \geq \text{b (under critical)} \\ 1 & , \frac{p_\text{d}}{p_\text{u}} \leq \text{b (over critical)} \end{cases} \tag{2.27}$$

where

$$\begin{aligned}
C &: \text{pneumatic conductance} \left[\frac{\text{kg}}{\text{s}}\right] \\
\rho &: \text{air density} \left[\frac{\text{kg}}{\text{m}^3}\right] \\
&\quad \rho = 1.293 \left[\frac{\text{kg}}{\text{m}^3}\right] \text{ for air (DIN 1306, 1984)} \\
\text{T}_0 &: \text{normed temperature 273.15[K] (DIN 1343, 1990)} \\
\psi &: \text{flow function} \\
p_\text{u} &: \text{entering flow pressure [Pa]} \\
p_\text{d} &: \text{exhausting flow pressure [Pa]} \\
\text{b} &: \text{critical pressure ratio between } p_\text{u} \text{ and } p_\text{d}
\end{aligned}$$

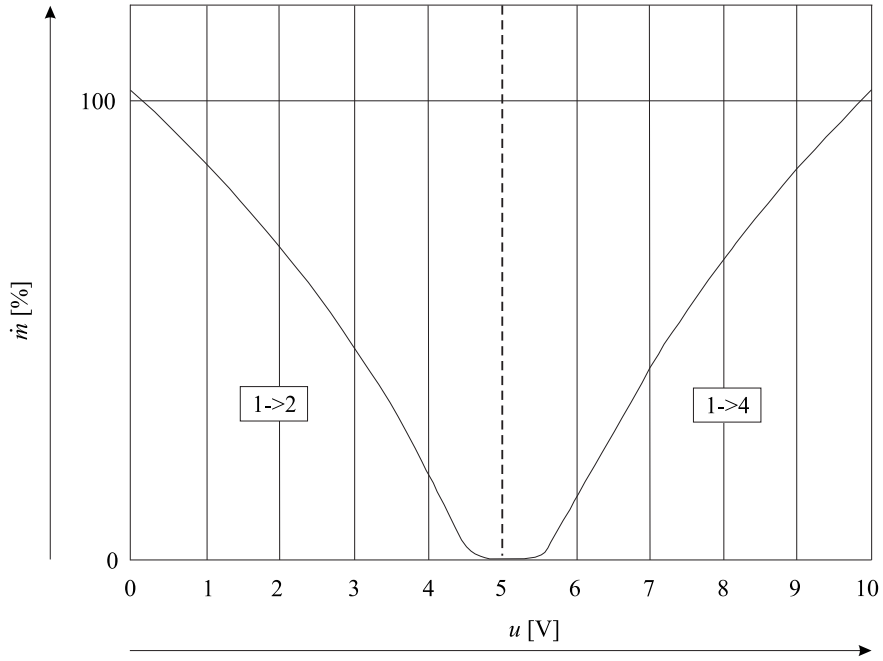

Figure 2.2: Conductance C related to a voltage

Figure 2.2 shows in graphical form the behavior of the conductance C in relationship to a voltage at it's entrance u, which regulates the mass flows $\dot{m}_1$ and $\dot{m}_2$ to the chambers. The two cases of the figure represent the relation of the entrance, related to the control voltage, to the two possible mass flows. That means, if u is lower than 5 V the supply connector 1 is connected to exit 2, otherwise air supply 1 is connected to exit 4.

Combining both equations (2.26) and (2.27) one obtains:

$$\dot{m} = \begin{cases} C\rho\sqrt{\frac{\mathrm{T}_0}{T}}p_\mathrm{u}\sqrt{1-\left(\frac{\left(\frac{p_\mathrm{d}}{p_\mathrm{u}}-b\right)}{1-b}\right)^2} & , \frac{p_\mathrm{d}}{p_\mathrm{u}} \geq \mathrm{b} \text{ (under critical)} \\ C\rho\sqrt{\frac{\mathrm{T}_0}{T}}p_\mathrm{u} & , \frac{p_\mathrm{d}}{p_\mathrm{u}} \leq \mathrm{b} \text{ (over critical)} \end{cases} \tag{2.28}$$

Figure 2.3 presents the flow of an ideal gas through an orifice. The velocity of the medium, in our case air, and the mass flow depend heavily on the values of the pressures p_u and p_d. If the relation of the both pressures is between the values of b to 1, (in our case 0.528, as it will be explained later), that means that the velocity of the medium is less than sonic velocity. This is defined as under critical. If in turn the value is less than b, then the gas reaches sonic velocity,

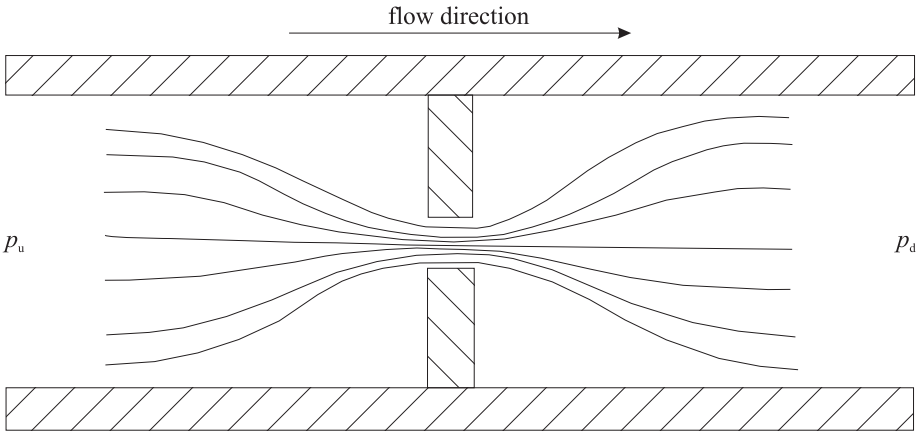

Figure 2.3: Airflow through an orifice

Table 2.1: Possible cases of mass flows (U - under critical / O - over critical)

	chamber 1		chamber 2	
	IN	OUT	IN	OUT
1	U	-	-	O
2	U	-	-	U
3	O	-	-	O
4	O	-	-	U
5	-	O	U	-
6	-	O	O	-
7	-	U	U	-
8	-	U	O	-

changes its behavior, while the mass flow is increasing. This case is defined as over critical. Both cases are shown in Figure 2.4.

The system owns eight different cases for the behavior of mass flows $\dot{m}_1$ and $\dot{m}_2$, as one can see in Table 2.1. Based on the design of the valve it is not possible to fill up or exhaust both chambers at the same time.

To keep the dynamic model as simple as possible, only the cases 1 and 5 of Table 2.1 are used because those are the only possibilities for the particular system under analysis. This is common praxis (Göttert and Neumann, 2007). It means that the exhaust always has the same value $\frac{p_d}{p_u}$ less than b, so over critical with medium velocities of sonic speed and filling the chambers is always under critical with the value $\frac{p_d}{p_u}$ grater than b.

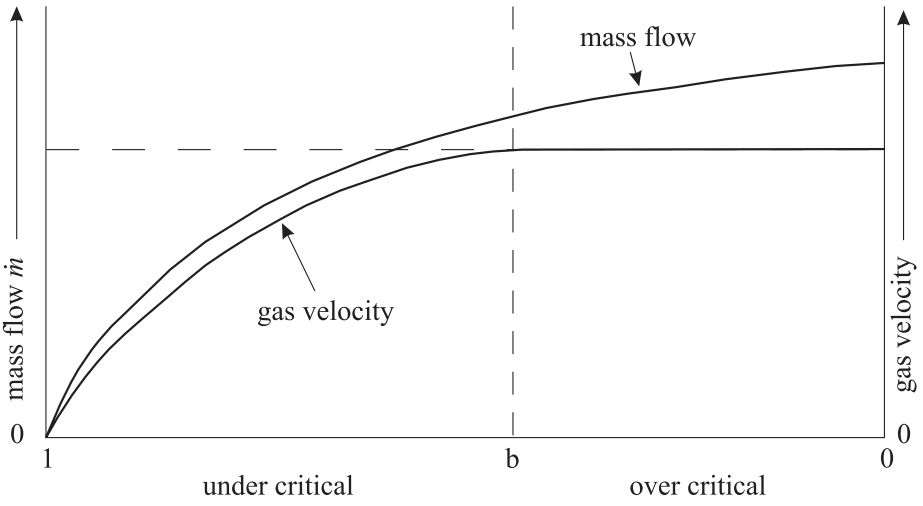

Figure 2.4: Critical pressure factor

The value of b is calculated as indicated in Beater (2007)

$$\mathrm{b} = \left(\frac{2}{\gamma+1}\right)^{\frac{\gamma+1}{\gamma-1}} = 0.528 \text{ (for air)} \tag{2.29}$$

This value can be used as a constant since it depends only on γ. Although this makes the analysis easier, care should be taken since b can actually vary from 0.125 to 0.9 (Beater, 2007). Using the value in this range above 0.528 implicates that the assumptions is that the system, in fact the valve, will not have problems with sub sonic velocities of the gas. Will be used a value under 0.528, it is assumed, that this will keep the system far away from sub sonic gas effects.

By taking into account the previous discussion and by assuming that $\sqrt{\frac{\mathrm{T}_0}{T}} = 1$ (because of working with air at a temperature T_0) y considering that the pneumatic conductance C is a non linear static function of u (with values between -1 and 1), equation (2.28) can be simplified to the following form

$$\dot{m} = \begin{cases} C(u)\rho p_{\mathrm{u}} \sqrt{1 - \left(\frac{\left(\frac{p_{\mathrm{d}}}{p_{\mathrm{u}}} - \mathrm{b}\right)}{1-\mathrm{b}}\right)^2} & , u \geq 0 \\ C(u)\rho p & , u \leq 0 \end{cases} \tag{2.30}$$

Or in the particular form of the system we get

$$\dot{m}_1 = \begin{cases} C(u)\rho \mathrm{p_s} \sqrt{1 - \left(\frac{\left(\frac{p_1}{\mathrm{p_s}} - \mathrm{b} \right)}{1 - \mathrm{b}} \right)^2} & , u \geq 0 \\ C(u)\rho p_1 & , u \leq 0 \end{cases} \tag{2.31}$$

$$\dot{m}_2 = \begin{cases} C(u)\rho p_2 & , u \geq 0 \\ C(u)\rho \mathrm{p_s} \sqrt{1 - \left(\frac{\left(\frac{p_2}{\mathrm{p_s}} - \mathrm{b} \right)}{1 - \mathrm{b}} \right)^2} & , u \leq 0 \end{cases} \tag{2.32}$$

where $\mathrm{p_s}$ = supply pressure [Pa].

2.3 Final dynamic model

Considering the equations (2.6), (2.24) and (2.25) and defining the state of the system as

$$\boldsymbol{x} = \begin{bmatrix} y \\ \dot{y} \\ p_1 \\ p_2 \end{bmatrix} = \begin{bmatrix} x_1 \\ x_2 \\ x_3 \\ x_4 \end{bmatrix} \tag{2.33}$$

one obtains the following state variable model

$$\dot{x}_1 = x_2 \tag{2.34}$$

$$\dot{x}_2 = \frac{\mathrm{A_1}}{\mathrm{M}} x_3 - \frac{\mathrm{A_2}}{\mathrm{M}} x_4 - \frac{\mathrm{A_1} - \mathrm{A_2}}{\mathrm{M}} \mathrm{p_{atm}} - \frac{F_\mathrm{v}}{\mathrm{M}} x_2 \tag{2.35}$$

$$\dot{x}_3 = \frac{\gamma}{\mathrm{V_{10}} + \mathrm{A_1} x_1} \left(\dot{m}_1(x_3, u) \mathrm{R_i T} - x_2 x_3 \mathrm{A_1} \right) \tag{2.36}$$

$$\dot{x}_4 = \frac{\gamma}{\mathrm{V_{20}} + \mathrm{A_2}(\mathrm{L} - x_1)} \left(\dot{m}_2(x_4, u) \mathrm{R_i T} - x_2 x_4 \mathrm{A_2} \right) \tag{2.37}$$

or in compact form

$$\sum := \begin{cases} \dot{\boldsymbol{x}} = \boldsymbol{f}(\boldsymbol{x}, u) & = \boldsymbol{a}(\boldsymbol{x}) + \boldsymbol{b}(\boldsymbol{x}, u) \\ \boldsymbol{z} = \boldsymbol{h}(\boldsymbol{x}) \end{cases} \tag{2.38}$$

with

$$\boldsymbol{a}(\boldsymbol{x}) = \begin{bmatrix} x_2 \\ \frac{\mathrm{A}_1}{\mathrm{M}} x_3 - \frac{\mathrm{A}_2}{\mathrm{M}} x_4 - \frac{\mathrm{A}_1 - \mathrm{A}_2}{\mathrm{M}} \mathrm{p_{atm}} - \frac{F_\mathrm{V}}{\mathrm{M}} x_2 \\ -\frac{\gamma x_2 x_3 \mathrm{A}_1}{\mathrm{V}_{10} + \mathrm{A}_1 x_1} \\ -\frac{\gamma x_2 x_4 \mathrm{A}_2}{\mathrm{V}_{20} + \mathrm{A}_2(\mathrm{L} - x_1)} \end{bmatrix} \tag{2.39}$$

$$\boldsymbol{b}(\boldsymbol{x}) = \begin{cases} \begin{bmatrix} 0 \\ 0 \\ \frac{\gamma \mathrm{R_i T} C(u) \rho \mathrm{p_s} \sqrt{1 - \left(\frac{\left(\frac{p_1}{\mathrm{p_s}} - \mathrm{b} \right)}{1 - \mathrm{b}} \right)^2}}{\mathrm{V}_{10} + \mathrm{A}_1 x_1} \\ \frac{\gamma \mathrm{R_i T} C(u) \rho p_2}{\mathrm{V}_{20} + \mathrm{A}_2(\mathrm{L} - x_1)} \end{bmatrix} & u > 0 \\ \begin{bmatrix} 0 \\ 0 \\ \frac{\gamma \mathrm{R_i T} C(u) \rho p_1}{\mathrm{V}_{10} + \mathrm{A}_1 x_1} \\ \frac{\gamma \mathrm{R_i T} C(u) \rho \mathrm{p_s} \sqrt{1 - \left(\frac{\left(\frac{p_2}{\mathrm{p_s}} - \mathrm{b} \right)}{1 - \mathrm{b}} \right)^2}}{\mathrm{V}_{20} + \mathrm{A}_2(\mathrm{L} - x_1)} \end{bmatrix} & u < 0 \end{cases} \tag{2.40}$$

$$\boldsymbol{h}(\boldsymbol{x}) = \begin{bmatrix} x_1 \\ 0 \\ x_3 \\ x_4 \end{bmatrix} \tag{2.41}$$

The $\boldsymbol{h}(\boldsymbol{x})$ represents all available states of the system.

2.4 Dynamic model (rewritten)

For further use, we redefine equations (2.31) and (2.32) to get:

$$\dot{m}_1 = C(u)\bar{\gamma}_1(x_3) \stackrel{\triangle}{=} C(u) \begin{cases} \rho_0 \mathrm{p_s} \sqrt{1 - \left(\frac{\left(\frac{x_3}{\mathrm{p_s}} - b \right)}{1-b} \right)^2} & u \geq 0 \text{ and } \frac{x_3}{\mathrm{p_s}} \geq b \\ \rho_0 \mathrm{p_s} & u \geq 0 \text{ and } \frac{x_3}{\mathrm{p_s}} < b \\ \rho_0 x_3 & u < 0 \end{cases} \tag{2.42}$$

and

$$\dot{m}_2 = -C(u)\bar{\gamma}_2(x_4) \stackrel{\triangle}{=} -C(u) \begin{cases} \rho_0 x_4 & u > 0 \\ \rho_0 \mathrm{p_s} \sqrt{1 - \left(\frac{\left(\frac{x_4}{\mathrm{p_s}} - b \right)}{1-b} \right)^2} & u \leq 0 \text{ and } \frac{x_4}{\mathrm{p_s}} \geq b \\ \rho_0 \mathrm{p_s} & u \leq 0 \text{ and } \frac{x_4}{\mathrm{p_s}} < b \end{cases} \tag{2.43}$$

Remark 1
The input voltage usually takes values from $0\,[V]$ *to* $+10\,[V]$*, but in (2.42)–(2.43) is considered that* $u \in (-5, +5)[V]$ *while a constant value* $V_{\text{offset}} \approx 5\,[V]$ *is added for implementation.* $\triangle$

Remark 2
The following physical facts hold:

1. $p_{\text{atm}} \leq x_3, x_4 \leq \mathrm{p_s}$
2. $0 \leq y \leq \mathrm{L}$
3. $\bar{\gamma}_1(x_3), \bar{\gamma}_2(x_4) \geq 0$ *and bounded*
4. $C(u)$ *is a strictly increasing function with* $C(0) = 0$

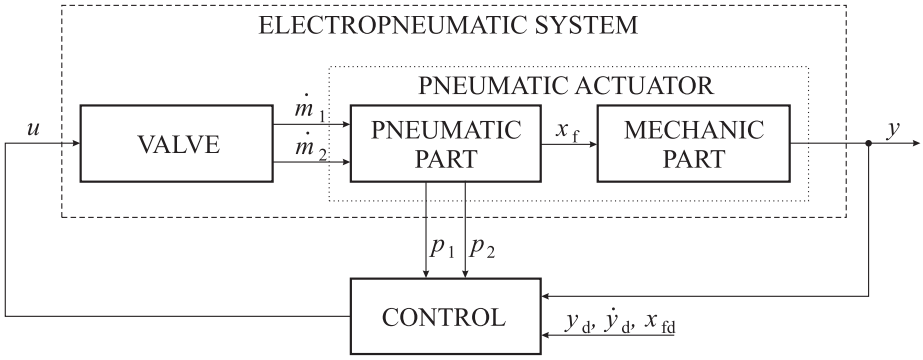

Figure 2.5: Description of the differential pneumatic actuator as two cascade systems

5. *There exists a constant* k_u *which fulfills*

$$|C(u)| > k_u|u| \tag{2.44}$$

△

For control design in Section 3.3 it will be convenient to rewrite model (2.33)–(2.43) according to the scheme proposed in Figure 2.5. This will allow to separate regulation of applied force and, as a result, piston position and velocity as well. In fact from equations (2.33)–(2.35) one gets

$$M\ddot{y} + F_V\dot{y} = x_f + p_{b1}, \tag{2.45}$$

where it is defined

$$x_f \triangleq A_1(x_3 - p_{atm}) - A_2(x_4 - p_{atm}), \tag{2.46}$$

and p_{b1} is a bounded perturbation that has been added for completeness of the model. The force x_f can be used as input for the mechanical subsystem. Its dynamics can be described by computing its derivative as

$$\begin{aligned}\dot{x}_f &= A_1\dot{x}_3 - A_2\dot{x}_4 \\ &= \frac{A_1\gamma RT}{V_{10} + A_1x_1}\dot{m}_1 - \frac{A_2\gamma RT}{V_{20} + A_2(L - x_1)}\dot{m}_2 \\ &\quad - \left(\frac{A_1^2\gamma x_3}{V_{10} + A_1x_1} - \frac{A_2^2\gamma x_4}{V_{20} + A_2(L - x_1)}\right)x_2.\end{aligned} \tag{2.47}$$

By taking into account (2.42)–(2.43) one can rewrite (2.47) as

$$\dot{x}_f = \bar{\gamma}(x_3, x_4)C(u) + b(t, x_3, x_4)x_2 \tag{2.48}$$

with

$$\bar{\gamma} = \frac{A_1 \gamma RT}{V_{10} + A_1 x_1} \bar{\gamma}_1(x_3) + \frac{A_2 \gamma RT}{V_{20} + A_2(L - x_1)} \bar{\gamma}_2(x_4) \tag{2.49}$$

and

$$b(t) = -\left(\frac{A_1^2 \gamma x_3}{V_{10} + A_1 x_1} - \frac{A_2^2 \gamma x_4}{V_{20} + A_2(L - x_1)} \right). \tag{2.50}$$

Finally, the system dynamics can be summarized also as

$$M\ddot{y} + F_V \dot{y} = x_{\mathrm{f}} + p_{\mathrm{b}1} \tag{2.51}$$

$$\dot{x}_{\mathrm{f}} = \bar{\gamma} C(u) + b(t)\dot{y} + p_{\mathrm{b}2}, \tag{2.52}$$

where we have included another bounded perturbation given by $p_{\mathrm{b}2}$. Note that according with Remark 2 both $\bar{\gamma}$ and $b(t)$ are bounded with $\bar{\gamma} > 0$.

Chapter 3

Control laws

As it has been shown in the introduction and in the previous chapter, computing an accurate model for differential pneumatic pistons may not be quite direct. Although it is possible to employ well–known identification algorithms to improve the mathematical description of the system (see for example Ioannou and Sun (1996)), for control purposes it may be more convenient to require little model information or none at all. In this section we intend to carry out an experimental comparison of different control laws with this property. In doing so many popular techniques like feedback linearization are excluded (see Khalil (2002)). For the same reason we do not consider some other related works. By taking into account the restriction of not using any dynamic model for implementation, we have chosen three algorithms: 1) The PID control because it is widely used for industrial applications. 2) A sliding mode technique because this kind of controllers are very robust against model uncertainties. 3) An adaptation of a robot control algorithm consisting in a combination of the other two techniques.

3.1 PID control

This is the most employed controller in industry and its structure is very well known:

$$u(t) = -\left(k_{\mathrm{p}} \cdot \Delta y(t) + k_{\mathrm{i}} \cdot \int_0^t \Delta y(\tau)\mathrm{d}\tau + k_{\mathrm{d}} \frac{\mathrm{d}\Delta y(t)}{\mathrm{d}t}\right), \tag{3.1}$$

where $\Delta y = y - y_{\mathrm{d}}$ and y_{d} is the desired trajectory which is assumed to be bounded and smooth. k_{p}, k_{i} and k_{d} are positive constants.

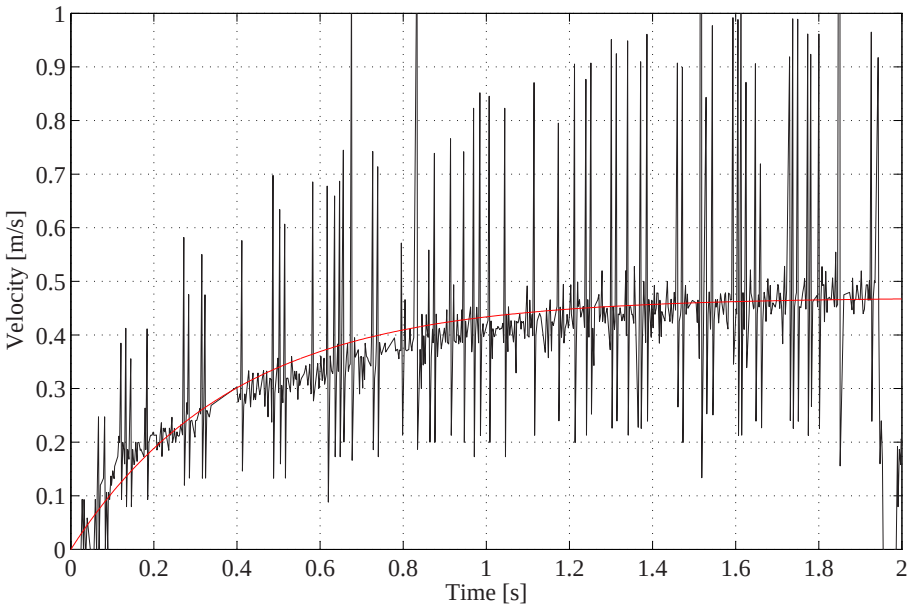

Figure 3.1: Step response for the test bed of Figure A.1 with $\dot{y}$ as output. (——) $\dot{y}$. (——) output of model (3.3).

3.2 Sliding mode controller

Sliding mode control is a technique that allows to cope with model uncertainties and disturbances. Since it turns out to be difficult for pneumatic actuators to get an accurate model, many controllers have been designed based on this approach (*e. g.* see Richer and Hurmuzlu (2000), Ning and Bone (2005), Shen *et al.* (2006) and Sobczyk and Perondi (2006)).

We have chosen the control law given in Ning and Bone (2005) because of its good performance. Note that this approach employs an input/output linear model given by

$$G(s) = \frac{Y(s)}{U(s)} = \frac{n_0}{s(s^2 + d_2 s + d_1)} \tag{3.2}$$

where $Y(s) = \mathcal{L}(y(t))$, $U(s) = \mathcal{L}(u(t))$ and $\mathcal{L}(\cdot)$ is the Laplace integral. However, the approximation is rough and we fairly consider this scheme qualifies as model free. In fact, to get n_0, d_2 and d_1 the step response for $\dot{y}(t)$ is calculated after experimentally measuring $y(t)$ to compute

$$G_{\dot{y}}(s) = \frac{\dot{Y}(s)}{U(s)} = \frac{n_0}{s^2 + d_2 s + d_1}. \tag{3.3}$$

The parameters obtained are $n_0 = 12051$, $d_2 = 10002.6$ and $d_1 = 25641$. The result can be seen in Figure 3.1. As could have been expected the actual $\dot{y}$ is

pretty noisy. For the control algorithm, the proposed sliding surface is

$$s = \ddot{y} - \ddot{y}_{\mathrm{d}} + 2\lambda(\dot{y} - \dot{y}_{\mathrm{d}}) + \lambda^2(y - y_{\mathrm{d}}) = \Delta\ddot{y} + 2\lambda\Delta\dot{y} + \lambda^2\Delta y, \tag{3.4}$$

where λ is chosen to make (3.4) Hurwitz. To achieve that the state reaches and stays in the sliding surface, the control signal is divided into two terms, u_{eq} and u_{s}, *i. e.*

$$u \quad = u_{\mathrm{eq}} + u_{\mathrm{s}} \tag{3.5}$$

with the switching control signal

$$u_{\mathrm{s}} \quad = -k_{\mathrm{s}}\mathrm{sat}\left(\frac{s}{\phi}\right) \tag{3.6}$$

where

$$\mathrm{sat}\left(\frac{s}{\phi}\right) = \begin{cases} \frac{s}{\phi} & \left|\frac{s}{\phi}\right| \leq 1 \\ \mathrm{sign}\left(\frac{s}{\phi}\right) & \left|\frac{s}{\phi}\right| > 1 \end{cases} \tag{3.7}$$

with $\mathrm{sign}(0) = 0$ and ϕ a positive constant. The equivalent control signal is

$$u_{\mathrm{eq}} \quad = \frac{1}{n_0}\left\{\dddot{y}_{\mathrm{d}} + d_2\ddot{y} + d_1\dot{y} - 2\lambda(\ddot{x} - \ddot{y}_{\mathrm{d}}) - \lambda^2(\dot{y} - \dot{y}_{\mathrm{d}})\right\}. \tag{3.8}$$

To obtain u_{eq}, it is taken into account that after (3.2) one has $\dddot{y} = -d_2\ddot{y} - d_1\dot{y} + n_0u$, and the derivative of (3.4) is computed to set $\dot{s} = 0$. See the reference for details.

3.3 Nonlinear PID with integrated sliding mode controller

Consider Figure 2.5 and equations (2.51)–(2.52). Clearly, (2.51) represents a one degree of freedom robot manipulator whose input is x_{f}. Thus, in principle any control algorithm for this kind of systems could employed. We have chosen that given in Arteaga-Pérez *et al.* (2006) because it can be utilized for (2.52) too, as will be shown in this section. First of all, in the reference a control–observer algorithm for robot manipulators is proposed that can be used directly for the

mechanical part as follows:

$$
\begin{aligned}
z &= y - \hat{y} && (3.9)\\
\dot{\hat{y}} &= \dot{y}_\mathrm{d} - \lambda_\mathrm{y}(\hat{y} - y_\mathrm{d}) + s_\mathrm{d} + k_\mathrm{d}\lambda_\mathrm{z}\int_0^t z(\vartheta)\mathrm{d}\vartheta + \lambda_\mathrm{z} z + k_\mathrm{d} z && (3.10)\\
s_\mathrm{y} &= \dot{\hat{y}} - \dot{y}_\mathrm{d} + \lambda_\mathrm{y}(\hat{y} - y_\mathrm{d}) \triangleq \dot{\bar{y}} + \lambda_\mathrm{y}\bar{y} && (3.11)\\
s_\mathrm{d} &= s_\mathrm{y}(0)e^{-kt} && (3.12)\\
s_{\mathrm{y}1} &= s_\mathrm{y} - s_\mathrm{d} && (3.13)\\
\sigma_\mathrm{y} &= \int_0^t \left(k_{\beta\mathrm{y}} s_{\mathrm{y}1}(\vartheta) + \mathrm{sign}\left(s_{\mathrm{y}1}(\vartheta)\right)\right)\mathrm{d}\vartheta \qquad \sigma_\mathrm{y}(0) = 0 && (3.14)\\
\dot{y}_\mathrm{r} &= \dot{y}_\mathrm{d} - \lambda_\mathrm{y}(\hat{y} - y_\mathrm{d}) + s_\mathrm{d} - k_{\gamma\mathrm{y}}\sigma_\mathrm{y} && (3.15)\\
\dot{y}_\mathrm{o} &= \dot{\hat{y}} - \lambda_\mathrm{z} z && (3.16)\\
s_\mathrm{o} &= \dot{y}_\mathrm{o} - \dot{y}_\mathrm{r}, && (3.17)
\end{aligned}
$$

where $\hat{y}$ is an estimated value for y, z is the observation error, Eq. (3.10) represents the observer, $s_\mathrm{y}, s_{\mathrm{y}1}$ are auxiliary sliding variables, s_d vanishes as time goes to infinity and is useful to get a better transient performance, σ_y is the integral term and $\dot{y}_\mathrm{r}$, $\dot{y}_\mathrm{o}$ and s_o are auxiliary variables to form the control law defined by

$$x_\mathrm{f} = -k_{\mathrm{py}} s_\mathrm{o}. \tag{3.18}$$

As shown in the reference, this control law guarantees that both observation and tracking error tend to zero, where the later is defined as

$$\Delta y = y - y_\mathrm{d}. \tag{3.19}$$

Now, we use a backstepping like approach as explained in Khalil (2002), so that in fact (3.18) is to be employed as a desired value for x_f in the form

$$x_\mathrm{fd} = -k_{\mathrm{py}} s_\mathrm{o}. \tag{3.20}$$

The next step is to design a control law for the pneumatic part of the system so that

$$x_\mathrm{f} \to x_\mathrm{fd} \qquad \text{or} \qquad \Delta x_\mathrm{f} \triangleq x_\mathrm{f} - x_\mathrm{fd} \to 0. \tag{3.21}$$

As explained before, we have chosen the control law in Arteaga-Pérez *et al.* (2006) because it can be used for this case too (without observer implementation). In fact, Eq. (2.52) can be rewritten as

$$\dot{x_\mathrm{f}} = \bar{\gamma} C(u) + b(t)\Delta\dot{y} + b(t)\dot{y}_\mathrm{d} + p_{\mathrm{b}2}, \tag{3.22}$$

and the control algorithm simply becomes

$$
\begin{aligned}
s_\mathrm{f} &= \Delta x_\mathrm{f} + k_{\gamma\mathrm{r}}\sigma_\mathrm{f} \;=\; x_\mathrm{f} - x_\mathrm{fd} + k_{\gamma\mathrm{r}}\sigma_\mathrm{f} && (3.23)\\
\sigma_\mathrm{f} &= \int_0^t \left(k_{\beta\mathrm{f}}\Delta x_\mathrm{f}(\vartheta) + \mathrm{sign}(\Delta x_\mathrm{f}(\vartheta))\right)\mathrm{d}\vartheta \qquad \sigma_\mathrm{f}(0) = 0 && (3.24)\\
u &= -k_{\mathrm{pf}} s_\mathrm{f} && (3.25)
\end{aligned}
$$

Thereby we get

$$\dot{x_{\mathrm{f}}} = \bar{\gamma}C(-k_{\mathrm{pf}}s_{\mathrm{f}}) + b(t)\Delta\dot{y} + \bar{p}_{\mathrm{b2}} \tag{3.26}$$

$$\bar{p}_{\mathrm{b2}} = b(t)\dot{y}_{\mathrm{d}} + p_{\mathrm{b2}}, \tag{3.27}$$

with $\bar{p}_{\mathrm{b2}}$ bounded.

Proposition 1
With a proper choice of gains, the control law of Eqs. (3.9)–(3.25) guarantees exact tracking for y, $\dot{y}$ and x_{f}. Additionally, the boundedness of every system signal is guaranteed. △

See Appendix B for the proof. Conditions for stability are also given.

Remark 3
As explained in Arteaga-Pérez et al. (2006), the control presented in this section represents a nonlinear PID with a second order sliding mode. △

Chapter 4

Observability analysis

The main goal of this chapter is to describe the manner to use the minimal number of sensors for the system, which has with 4 states: $y, \dot{y}, p_1, p_2$. Generally 3 principal sensors are used, one for the displacement y and two for the pressures in the chambers of the piston, p_1 and p_2. Based on this measurements these states are available. To determine if it is possible to estimate one of the system states, it's necessary to carry out a series of analysis. Based on Table 2.1, we will consider only the first case, which is the most important and common one. Developing this analysis we use the scheme shown in Table 4.1, including the number of available states.

Case	Available			Non Available			
	y	p_1	p_2	y	$\dot{y}$	p_1	p_2
1	y				$\dot{y}$	p_1	p_2
2		p_1		y	$\dot{y}$		p_2
3			p_2	y	$\dot{y}$	p_1	
4	y	p_1			$\dot{y}$		p_2
5	y		p_2		$\dot{y}$	p_1	
6		p_1	p_2	y	$\dot{y}$		

Table 4.1: Complete Analysis Scheme

As can be seen, six different cases for an observability analysis should be considered. On the other hand, since there is no difference whether pressure p_1 or p_2 is given, we can reduce the analysis to 4 cases as shown in Table 4.2.

4.1 Observability analysis with y available

In Wu *et al.* (2003) the authors already studied the observability, based on the proposed rank condition test published in Hermann and Kerner (1977), of the

Case	Available			Non Available			
	y	p_1	p_2	y	$\dot{y}$	p_1	p_2
1	y				$\dot{y}$	p_1	p_2
2		p_1		y	$\dot{y}$		p_2
3	y	p_1			$\dot{y}$		p_2
4		p_1	p_2	y	$\dot{y}$		

Table 4.2: Compact Analysis Scheme

system assuming that the only available state is the displacement y (Case 1 of Table 4.2), what means

$$z = \begin{bmatrix} 1 & 0 & 0 & 0 \end{bmatrix} \begin{bmatrix} y \\ \dot{y} \\ p_1 \\ p_2 \end{bmatrix} = y \tag{4.1}$$

or expressed in x

$$z = \begin{bmatrix} 1 & 0 & 0 & 0 \end{bmatrix} \begin{bmatrix} x_1 \\ x_2 \\ x_3 \\ x_4 \end{bmatrix} = x_1 \tag{4.2}$$

and as output function of the system one gets

$$h_1(\boldsymbol{x}) = \begin{bmatrix} x_1 & 0 & 0 & 0 \end{bmatrix}. \tag{4.3}$$

By considering that while one chamber is filling up in an under critical state, the other one is evacuating in a over critical state and based on rewriting equations (2.34) to (2.37) as vector $\boldsymbol{f}$ we get

$$\boldsymbol{f} = \begin{bmatrix} x_2 \\ \dfrac{\mathrm{A}_1}{\mathrm{M}} x_3 - \dfrac{\mathrm{A}_2}{\mathrm{M}} x_4 - \dfrac{\mathrm{A}_1 - \mathrm{A}_2}{\mathrm{M}} \mathrm{p_{atm}} - \dfrac{F_\mathrm{v}}{\mathrm{M}} x_2 \\ -\dfrac{\gamma}{\mathrm{V}_{10} + \mathrm{A}_1 x_1} \left(\dot{m}_1 \mathrm{R_i T} - x_2 x_3 \mathrm{A}_1 \right) \\ \dfrac{\gamma}{\mathrm{V}_{20} + \mathrm{A}_2 (\mathrm{L} - x_1)} \left(\dot{m}_2 \mathrm{R_i T} - x_2 x_4 \mathrm{A}_2 \right) \end{bmatrix} \tag{4.4}$$

For further use, the partial derivative of $\boldsymbol{f}$ is

$$\frac{\partial \boldsymbol{f}}{\partial x} = \begin{bmatrix} pf_{11} & pf_{12} & pf_{13} & pf_{14} \\ pf_{21} & pf_{22} & pf_{23} & pf_{24} \\ pf_{31} & pf_{32} & pf_{33} & pf_{34} \\ pf_{41} & pf_{42} & pf_{43} & pf_{44} \end{bmatrix} \tag{4.5}$$

$$\begin{bmatrix} pf_{11} \\ pf_{21} \\ pf_{31} \\ pf_{41} \end{bmatrix} = \begin{bmatrix} 0 \\ 0 \\ \dfrac{(\gamma\, \dot{m}_1 \mathrm{R_i T A_1}) - (\gamma\, x_2 x_3 {\mathrm{A_1}}^2)}{(\mathrm{V_{10}} + \mathrm{A_1} x_1)^2} \\ \dfrac{\left(\gamma\, \dot{m}_2 \mathrm{R_i T A_2 (L} - x_1)\right) - \left(\gamma\, x_2 x_4 {\mathrm{A_2}}^2 (\mathrm{L} - x_1)\right)}{\left(\mathrm{V_{20}} + \mathrm{A_2 (L} - x_1)\right)^2} \end{bmatrix} \tag{4.6}$$

$$\begin{bmatrix} pf_{12} \\ pf_{22} \\ pf_{32} \\ pf_{42} \end{bmatrix} = \begin{bmatrix} 1 \\ -\dfrac{F_\mathrm{v}}{\mathrm{M}} \\ \dfrac{\gamma\, x_3 \mathrm{A_1}}{\mathrm{V_{10}} + \mathrm{A_1} x_1} \\ -\dfrac{\gamma\, x_4 A_2}{\mathrm{V_{20}} + \mathrm{A_2 (L} - x_1)} \end{bmatrix} \tag{4.7}$$

$$\begin{bmatrix} pf_{13} \\ pf_{23} \\ pf_{33} \\ pf_{43} \end{bmatrix} = \begin{bmatrix} 0 \\ \dfrac{\mathrm{A_1}}{\mathrm{M}} \\ \dfrac{\gamma\, x_2 \mathrm{A_1}}{\mathrm{V_{10}} + \mathrm{A_1} x_1} \\ 0 \end{bmatrix} \tag{4.8}$$

$$\begin{bmatrix} pf_{14} \\ pf_{24} \\ pf_{34} \\ pf_{44} \end{bmatrix} = \begin{bmatrix} 0 \\ -\dfrac{\mathrm{A_2}}{\mathrm{M}} \\ 0 \\ -\dfrac{\gamma\, x_2 \mathrm{A_2}}{\mathrm{V_{20}} + \mathrm{A_2 (L} - x_1)} \end{bmatrix} \tag{4.9}$$

Now by partial differentiation of equation (4.3) one gets the first Lie Derivative

$$L^0_{\boldsymbol{f}} \mathrm{d}h_1 = \frac{\partial h_1}{\partial x} = \begin{bmatrix} 1 & 0 & 0 & 0 \end{bmatrix} \tag{4.10}$$

The second Lie Derivative is calculated by

$$L^1_{\boldsymbol{f}} \mathrm{d}h_1 = \frac{\partial h_1}{\partial x} \frac{\partial \boldsymbol{f}}{\partial x} + \left[\frac{\partial}{\partial x} \left(\frac{\partial h_1}{\partial x} \right)^T \boldsymbol{f} \right]^T \tag{4.11}$$

$$= \begin{bmatrix} 0 & 1 & 0 & 0 \end{bmatrix} + \begin{bmatrix} 0 & 0 & 0 & 0 \end{bmatrix} \tag{4.12}$$

$$= \begin{bmatrix} 0 & 1 & 0 & 0 \end{bmatrix} \tag{4.13}$$

The third by

$$L^2_{\boldsymbol{f}}\mathrm{d}h_1 = L^1_f dh_1 \frac{\partial \boldsymbol{f}}{\partial x} + \left[\frac{\partial}{\partial x}\left(L^1_{\boldsymbol{f}}\mathrm{d}h_1\right)^T \boldsymbol{f}\right]^T \tag{4.14}$$

$$= \begin{bmatrix} 0 & -\frac{F_\mathrm{v}}{\mathrm{M}} & \frac{\mathrm{A}_1}{\mathrm{M}} & -\frac{\mathrm{A}_2}{\mathrm{M}} \end{bmatrix} + \begin{bmatrix} 0 & 0 & 0 & 0 \end{bmatrix} \tag{4.15}$$

$$= \begin{bmatrix} 0 & -\frac{F_\mathrm{v}}{\mathrm{M}} & \frac{\mathrm{A}_1}{\mathrm{M}} & -\frac{\mathrm{A}_2}{\mathrm{M}} \end{bmatrix} \tag{4.16}$$

And the forth in the same manner

$$L^3_{\boldsymbol{f}}\mathrm{d}h_1 = L^2_f dh_1 \frac{\partial \boldsymbol{f}}{\partial x} + \left[\frac{\partial}{\partial x}\left(L^2_{\boldsymbol{f}}\mathrm{d}h_1\right)^T \boldsymbol{f}\right]^T \tag{4.17}$$

$$= \begin{bmatrix} L_{41} & L_{42} & L_{43} & L_{44} \end{bmatrix} + \begin{bmatrix} 0 & 0 & 0 & 0 \end{bmatrix} \tag{4.18}$$

$$= \begin{bmatrix} L_{41} & L_{42} & L_{43} & L_{44} \end{bmatrix} \tag{4.19}$$

with

$$L_{41} = \frac{(\gamma\, \dot{m}_1 \mathrm{R_i T {A_1}^2}) - (\gamma\, x_2 x_3 {\mathrm{A_1}^3})}{\mathrm{M}(\mathrm{V}_{10} + \mathrm{A}_1 x_1)^2} - \frac{\left(\gamma\, \dot{m}_2 \mathrm{R_i T {A_2}^2(L} - x_1)\right) - \left(\gamma\, x_2 x_4 {\mathrm{A_2}^3(L} - x_1)\right)}{\mathrm{M}\left(\mathrm{V}_{20} + \mathrm{A}_2(\mathrm{L} - x_1)\right)^2} \tag{4.20}$$

$$L_{42} = \frac{{F_\mathrm{v}}^2}{\mathrm{M}^2} + \frac{{\mathrm{A}_1}^2 \gamma\, x_3}{\mathrm{M}(\mathrm{V}_{10} + \mathrm{A}_1 x_1)} + \frac{{\mathrm{A}_2}^2 \gamma\, x_4}{\mathrm{M}(\mathrm{V}_{20} + \mathrm{A}_2(\mathrm{L} - x_1))} \tag{4.21}$$

$$L_{43} = -\frac{F_\mathrm{v}\mathrm{A}_1}{\mathrm{M}^2} + \frac{{\mathrm{A}_1}^2 \gamma\, x_2}{\mathrm{M}(\mathrm{V}_{10} + \mathrm{A}_1 x_1)} \tag{4.22}$$

$$L_{44} = \frac{F_\mathrm{v}\mathrm{A}_2}{\mathrm{M}^2} + \frac{{\mathrm{A}_2}^2 \gamma\, x_2}{\mathrm{M}(\mathrm{V}_{20} + \mathrm{A}_2(\mathrm{L} - x_1))} \tag{4.23}$$

The observability matrix is composed of the four Lie Derivatives, equations (4.10), (4.13), (4.16) and (4.19), and given in the form:

$$K_1 = \begin{bmatrix} L^0_{\boldsymbol{f}}\mathrm{d}h_1 \\ L^1_{\boldsymbol{f}}\mathrm{d}h_1 \\ L^2_{\boldsymbol{f}}\mathrm{d}h_1 \\ L^3_{\boldsymbol{f}}\mathrm{d}h_1 \end{bmatrix} = \begin{bmatrix} 1 & 0 & 0 & 0 \\ 0 & 1 & 0 & 0 \\ 0 & -\frac{F_\mathrm{v}}{\mathrm{M}} & \frac{\mathrm{A}_1}{\mathrm{M}} & -\frac{\mathrm{A}_2}{\mathrm{M}} \\ L_{41} & L_{42} & L_{43} & L_{44} \end{bmatrix} \tag{4.24}$$

Based on Hermann and Kerner (1977), the observability matrix K_1 has to be a full rank matrix to fulfill the condition of local weak observability. This

will not be the case when:

$$\frac{\mathrm{A}_1}{\mathrm{M}} L_{44} \neq -\frac{\mathrm{A}_2}{\mathrm{M}} L_{43} \tag{4.25}$$

$$\left(\frac{\mathrm{A}_1}{\mathrm{M}}\right)\left(\frac{F_\mathrm{v}\mathrm{A}_2}{\mathrm{M}^2} + \frac{{\mathrm{A}_2}^2\gamma x_2}{\mathrm{M}(\mathrm{V}_{20} + \mathrm{A}_2(\mathrm{L} - x_1))}\right) \neq \left(-\frac{\mathrm{A}_2}{\mathrm{M}}\right)\left(-\frac{F_\mathrm{v}\mathrm{A}_1}{\mathrm{M}^2} + \frac{{\mathrm{A}_1}^2\gamma x_2}{\mathrm{M}(\mathrm{V}_{10} + \mathrm{A}_1 x_1)}\right) \tag{4.26}$$

Analyzing the equation (4.26) it's possible to drawn the conclusion that the system will loose observability if $x_2 = 0$, what means that the velocity of the system is zero. Because of this the system is not observable if the only available state will be y.

4.2 Observability analysis with p_1 or p_2 available

To determine whether the system is observable if the only available state is p_1 (Case 2 of Table 4.2), the approach described in Zeitz (1984) will be used, consisting in trying to rewrite y (x_1), $\dot{y}$ (x_2) and p_2 (x_4) only as a function of p_1 (x_3) and its derivatives. At first we have to factorize x_2 of equation (2.36):

$$\begin{aligned}
\dot{x}_3 &= \frac{\gamma}{\mathrm{V}_{10} + \mathrm{A}_1 x_1}\left(\dot{m}_1(x_3, u)\mathrm{R_i T} - x_2 x_3 \mathrm{A}_1\right) \\
\dot{x}_3 &= \frac{\gamma\, \dot{m}_1(x_3, u)\mathrm{R_i T}}{\mathrm{V}_{10} + \mathrm{A}_1 x_1} - \frac{\gamma x_2 x_3 \mathrm{A}_1}{\mathrm{V}_{10} + \mathrm{A}_1 x_1} \\
\frac{\gamma x_2 x_3 \mathrm{A}_1}{\mathrm{V}_{10} + \mathrm{A}_1 x_1} &= \frac{\gamma\, \dot{m}_1(x_3, u)\mathrm{R_i T}}{\mathrm{V}_{10} + \mathrm{A}_1 x_1} - \dot{x}_3 \\
\gamma x_2 x_3 \mathrm{A}_1 &= \frac{\gamma\, \dot{m}_1(x_3, u)\mathrm{R_i T}\,(\mathrm{V}_{10} + \mathrm{A}_1 x_1)}{\mathrm{V}_{10} + \mathrm{A}_1 x_1} - \dot{x}_3(\mathrm{V}_{10} + \mathrm{A}_1 x_1)
\end{aligned}$$

what leads us to:

$$x_2 = \frac{\dot{m}_1(x_3, u)\mathrm{R_i T}}{x_3 A_1} - \frac{\dot{x_3}(V_{10} + A_1 x_1)}{\gamma x_3 A_1} \tag{4.27}$$

As can be appreciated x_2 is a function of x_1 and x_3. To eliminate x_1 it is possible to differentiate and substitute $\dot{x_2}$ from (2.35). Nevertheless, by differentiating (4.27) one gets $\dot{x}_1 = x_2$. Additionally $\dot{x_2}$ in (2.35) depends on x_4 and x_2 which are not available. Although we could continue infinitely, we can conclude, that $\dot{x_2}$ always will be a function of x_2 and that it is not possible to describe this state only as a function of p_1. By this fact, the system is not observable if only one of the pressures of the both chambers is measured.

4.3 Observability analysis with p_1 and p_2 available

In this case it has to be possible to rewrite x_1 and x_2 (Case 3 of Table 4.2) as a function of only x_3, x_4 and it's derivatives. Still, in case of $\dot{x}_1 = x_2$, indeed we have to try to express x_1 as function of x_3, x_4 and it's derivatives. This is only possible by combining (2.36) and (2.37).

$$x_1 = \frac{\gamma}{\mathrm{A}_1\dot{x_3}}\left(\dot{m}_1\mathrm{R_i T} - x_2x_3\mathrm{A}_1\right) - \frac{\mathrm{V}_{10}}{\mathrm{A}_1} \tag{4.28}$$

$$x_1 = -\frac{\gamma}{\mathrm{A}_2\dot{x_4}}\left(\dot{m}_2\mathrm{R_i T} - x_2x_4\mathrm{A}_2\right) + \frac{\mathrm{V}_{20}}{\mathrm{A}_2} + \mathrm{L} \tag{4.29}$$

$$-\frac{\gamma}{\mathrm{A}_2x_4}\left(\dot{m}_2\mathrm{R_i T} - x_2x_4\mathrm{A}_2\right) + \frac{\mathrm{V}_{20}}{\mathrm{A}_2} + \mathrm{L} = \frac{\gamma}{\mathrm{A}_1x_3}\left(\dot{m}_1\mathrm{R_i T} - x_2x_3\mathrm{A}_1\right) - \frac{\mathrm{V}_{10}}{\mathrm{A}_1}$$

$$\frac{x_2x_4\gamma}{\dot{x_4}} + \frac{x_2x_3\gamma}{\dot{x_3}} = \frac{\gamma}{\mathrm{A}_2\dot{x_4}}\left(\dot{m}_2\mathrm{R_i T}\right) + \frac{\gamma}{\mathrm{A}_1\dot{x_3}}\left(\dot{m}_1\mathrm{R_i T}\right) - \frac{\mathrm{V}_{10}}{\mathrm{A}_1} - \frac{\mathrm{V}_{20}}{\mathrm{A}_2} - \mathrm{L}$$

$$x_2\left(\frac{x_4\dot{x_3} + x_3\dot{x_4}}{\dot{x_3}\dot{x_4}}\right) = \mathrm{R_i T}\left(\frac{\mathrm{A}_1\dot{m}_2\dot{x_3} + \mathrm{A}_2\dot{m}_1\dot{x_4}}{\mathrm{A}_1\mathrm{A}_2\dot{x_3}\dot{x_4}}\right) - \frac{\mathrm{V}_{10}}{\mathrm{A}_1\gamma} - \frac{\mathrm{V}_{20}}{\mathrm{A}_2\gamma} - \frac{\mathrm{L}}{\gamma}$$

$$x_2 = \mathrm{R_i T}\left(\frac{\mathrm{A}_1\dot{m}_2\dot{x_3} + \mathrm{A}_2\dot{m}_1\dot{x_4}}{\mathrm{A}_1\mathrm{A}_2(x_4\dot{x_3} + x_3\dot{x_4})}\right) - \left(\frac{\mathrm{V}_{10}}{\mathrm{A}_1\gamma} - \frac{\mathrm{V}_{20}}{\mathrm{A}_2\gamma} - \frac{\mathrm{L}}{\gamma}\right)\frac{\dot{x_3}\dot{x_4}}{x_4\dot{x_3} + x_3\dot{x_4}} \tag{4.30}$$

Replacing the obtained equation (4.30) for x_2 in (4.28)

$$\begin{aligned} x_1 = \frac{\gamma}{\mathrm{A}_1\dot{x_3}}\Bigg(&\dot{m}_1\mathrm{R_i T} - \mathrm{R_i T}\left(\frac{\mathrm{A}_1\dot{m}_2\dot{x_3} + \mathrm{A}_2\dot{m}_1\dot{x_4}}{\mathrm{A}_1\mathrm{A}_2(x_4\dot{x_3} + x_3\dot{x_4})}\right) \\ &- \left(\frac{\mathrm{V}_{10}}{\mathrm{A}_1\gamma} - \frac{\mathrm{V}_{20}}{\mathrm{A}_2\gamma} - \frac{\mathrm{L}}{\gamma}\right)\frac{\dot{x_3}\dot{x_4}}{x_4\dot{x_3} + x_3\dot{x_4}}x_3\mathrm{A}_1\Bigg) - \frac{\mathrm{V}_{10}}{\mathrm{A}_1} \end{aligned}$$

or (4.29)

$$\begin{aligned} x_1 = -\frac{\gamma}{\mathrm{A}_2\dot{x_4}}\Bigg(&\dot{m}_2\mathrm{R_i T} - \mathrm{R_i T}\left(\frac{\mathrm{A}_1\dot{m}_2\dot{x_3} + \mathrm{A}_2\dot{m}_1\dot{x_4}}{\mathrm{A}_1\mathrm{A}_2(x_4\dot{x_3} + x_3\dot{x_4})}\right) \\ &- \left(\frac{\mathrm{V}_{10}}{\mathrm{A}_1\gamma} - \frac{\mathrm{V}_{20}}{\mathrm{A}_2\gamma} - \frac{\mathrm{L}}{\gamma}\right)\frac{\dot{x_3}\dot{x_4}}{x_4\dot{x_3} + x_3\dot{x_4}}x_4\mathrm{A}_2\Bigg) + \frac{\mathrm{V}_{20}}{\mathrm{A}_2} + \mathrm{L} \end{aligned}$$

we get the value of x_1. Nevertheless the system will not be observable if $\dot{x_3} = \dot{x_4} = 0$, which is a real common case, what is equivalent for p_1 and p_2 to be constant.

4.4 Observability analysis with y and p_1 or p_2 available

At last we analyze the observability of the system if y (x_1) and p_1 (x_3) (or $p_2 = x_4$) are available (Case 4 of Table 4.2). Clearly x_2 is a function of x_1 and it's derivatives out of the definition $\dot{x}_1 = x_2$. So we need to determine if it's possible to rewrite x_4 only as a function of x_1, x_3 and it's derivatives. What is obtained directly from (2.35)

$$x_4 = \frac{\mathrm{A}_1}{\mathrm{A}_2} x_3 - \frac{\mathrm{A}_1 - \mathrm{A}_2}{\mathrm{A}_2} \mathrm{p}_{\mathrm{atm}} - \frac{F_{\mathrm{V}}}{\mathrm{A}_2} x_2 - \frac{M}{\mathrm{A}_2} \dot{x_2} \tag{4.31}$$

Based on the previous we can conclude that in this case the system is observable. Alternatively when x_4 is the available state instead of x_3 we get again from (2.35)

$$x_3 = \frac{\mathrm{A}_2}{\mathrm{A}_1} x_4 + \frac{\mathrm{A}_1 - \mathrm{A}_2}{\mathrm{A}_1} \mathrm{p}_{\mathrm{atm}} + \frac{F_{\mathrm{V}}}{\mathrm{A}_1} x_2 + \frac{M}{\mathrm{A}_1} \dot{x_2} \tag{4.32}$$

So, the system is observable in this case, as could have been expected.

Remark 4 *As a lack of time the shown observability analysis is not used for the design of an observer in this work.*

Chapter 5

Experimental comparison of non model based control algorithms

In this Chapter we carry out the implementation of the control laws given in Chapter 3. We have chosen six different trajectories to test them under many conditions:

$$y_{d1}(t) = 0.28\sin(0.1 \cdot 2\pi t) + 0.38 \qquad y(0) = 0.38 \text{ [m]} \quad (5.1)$$
$$y_{d2}(t) = 0.28\sin(0.2 \cdot 2\pi t) + 0.38 \qquad y(0) = 0.38 \text{ [m]} \quad (5.2)$$
$$y_{d3}(t) = 0.028\sin(0.1 \cdot 2\pi t) + 0.38 \qquad y(0) = 0.38 \text{ [m]} \quad (5.3)$$
$$y_{d4}(t) = 0.028\sin(0.2 \cdot 2\pi t) + 0.38 \qquad y(0) = 0.38 \text{ [m]} \quad (5.4)$$
$$y_{d5}(t) = 0.28\,\text{square}(0.2 \cdot 2\pi t) + 0.38 \qquad y(0) = 0.10 \text{ [m]} \quad (5.5)$$
$$y_{d6}(t) = 0.028\,\text{square}(0.2 \cdot 2\pi t) + 0.38 \qquad y(0) = 0.35 \text{ [m]} \quad (5.6)$$

Desired trajectories $y_{d1}(t)$ to $y_{d6}(t)$ have been chosen to cope with almost the entire work space of the piston, whose length is L = 0.76[m]. Although only two frequencies have been chosen, by using square waves as desired trajectories the response of the system to fast movements is tested[1]. On the other hand, chosen trajectories help to show up expected friction effects in the different cases. We have taken care that the trajectories are reachable with the given supply pressure $p_s = 2 \cdot 10^5$Pa.

Since our goal is to get the better possible results for every trajectory, we have chosen to tune gains slightly different in some cases to improve performance for each algorithm. Table 5.1 shows the parameters for the PID and Table 5.2 those for the Sliding Mode Algorithm. Recall that the model in (3.3) has to be the same for all cases. Finally, for the algorithm of Section 3.3 the gains are

[1]Note that the square wave is not a smooth signal. For this reason it is a more demanding task than the test signal used in Ning and Bone (2005).

Trajectory	k_p	k_i	k_d
$y_{\mathrm{d}1}$	65	0.5	0.05
$y_{\mathrm{d}2}$	100	0.5	0.05
$y_{\mathrm{d}3}$	65	0.5	0.05
$y_{\mathrm{d}4}$	65	0.5	0.05
$y_{\mathrm{d}5}$	150	0.5	0.2
$y_{\mathrm{d}6}$	150	0.5	0.2

Table 5.1: Parameters for the PID control law

Trajectory	λ	k_s	ϕ
$y_{\mathrm{d}1}$	2500	120	4
$y_{\mathrm{d}2}$	3500	120	4
$y_{\mathrm{d}3}$	2500	120	4
$y_{\mathrm{d}4}$	3500	120	4
$y_{\mathrm{d}5}$	3500	120	4
$y_{\mathrm{d}6}$	3500	120	4

Table 5.2: Parameters for the sliding mode control law

given in Table 5.3. To tune these parameters it is advisable to set first $k_{\beta\mathrm{f}} = 0$, $k_{\beta\mathrm{y}} = 0$, $k_{\gamma\mathrm{f}} = 0$ and $k_{\gamma\mathrm{y}} = 0$ until a good enough behavior is obtained and then used the rest of gains to get better results.

Trajectory	$k_{\beta\mathrm{f}}$	$k_{\beta\mathrm{y}}$	$k_{\gamma\mathrm{f}}$	$k_{\gamma\mathrm{y}}$	k_{py}	λ_y	λ_z	k_d	k	k_{pf}
$y_{\mathrm{d}1}$	5	150	0.01	0.03	50	200	125	350	1	0.025
$y_{\mathrm{d}2}$	5	150	0.01	0.03	95	200	125	350	1	0.025
$y_{\mathrm{d}3}$	5	150	0.01	0.03	50	200	125	350	1	0.025
$y_{\mathrm{d}4}$	5	150	0.01	0.03	50	200	125	350	1	0.025
$y_{\mathrm{d}5}$	15	15	$5 \cdot 10^{-5}$	$5 \cdot 10^{-7}$	100	200	125	350	1	0.025
$y_{\mathrm{d}6}$	15	15	$5 \cdot 10^{-5}$	$5 \cdot 10^{-7}$	80	200	125	350	1	0.025

Table 5.3: Parameters for the algorithm of Section 3.3

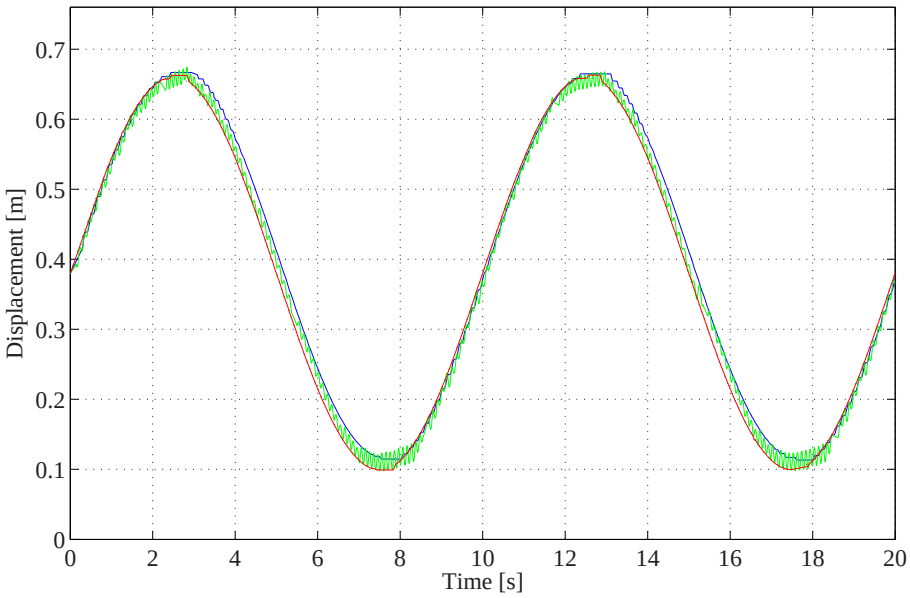

Figure 5.1: Experimental results for $y_{\mathrm{d}1}(t)$. $(\cdots)$ Desired trajectory. (——) PID Control. (——) Sliding mode control. (——) Control algorithm of Section 3.3.

5.1 Experimental results for $y_{\mathrm{d}1}(t)$

For the first desired trajectory the results in tracking are shown in Figure 5.1. It can be appreciated that the proposed scheme of Section 3.3 works better while the PID and the sliding mode control deliver similar outcomes. We note that the movement is wide but not too fast. In Figure 5.2 tracking errors are shown. To have a more objective insight, in Section 5.7 we have computed the root mean square errors as suggested by Ning and Bone (2005). The outcomes can be seen in Table 5.4, where it can be appreciated that in fact the algorithm of Section 3.3 works much better. Figure 5.3 shows the input voltages u. Not surprisingly, the sliding mode controller shows chattering. Note that the third algorithm avoids this problem by using the sign function within the integral term. Quite interesting, the input voltage for the PID is very similar. Another important aspect to take into account is the pressure in each chamber (see Figure 5.4). While they are different for each case, in none of them the supply pressure $\mathrm{p_s}$ is reached, so that the behavior is acceptable. Also, the observer error $z = y - \hat{y}$ formed only for the last scheme is shown in Figure 5.5.

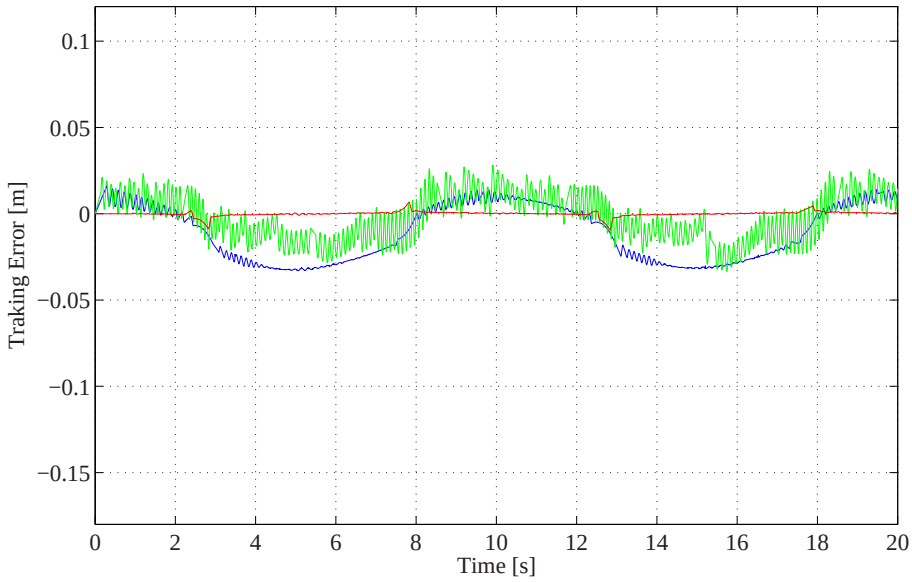

Figure 5.2: Experimental results for $y_{\mathrm{d}1}(t)$. Tracking error Δy. (——) PID Control. (——) Sliding mode control. (——) Control algorithm of Section 3.3.

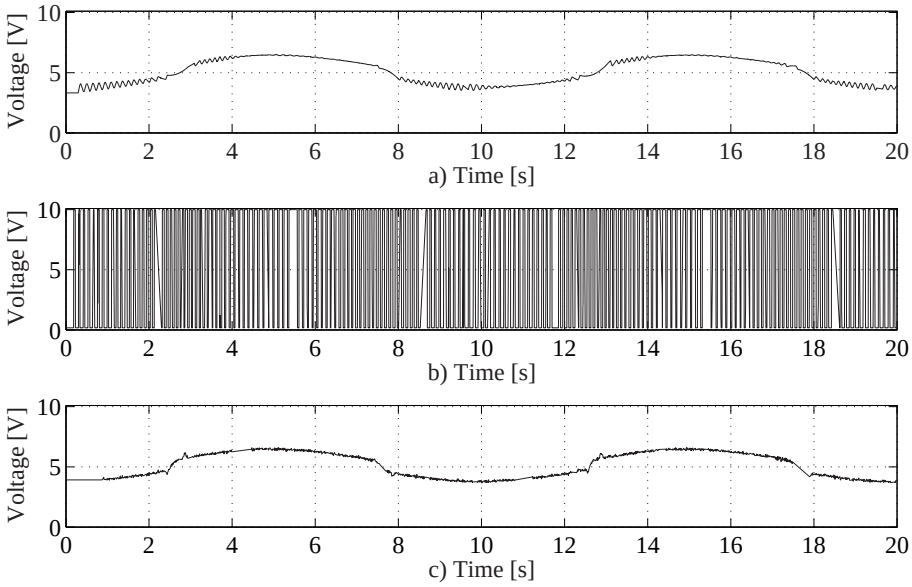

Figure 5.3: Experimental results for $y_{\mathrm{d}1}(t)$. Input voltage u. a) PID Control. b) Sliding mode control. c) Control algorithm of Section 3.3.

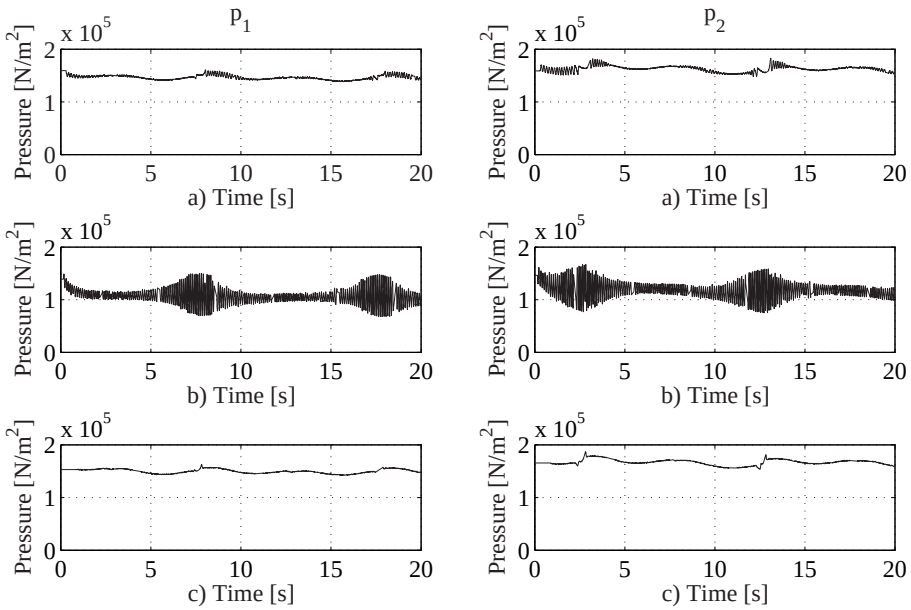

Figure 5.4: Experimental results for $y_{\mathrm{d}1}(t)$. Pressures in chambers 1 and 2. a) PID Control. b) Sliding mode control. c) Control algorithm of Section 3.3.

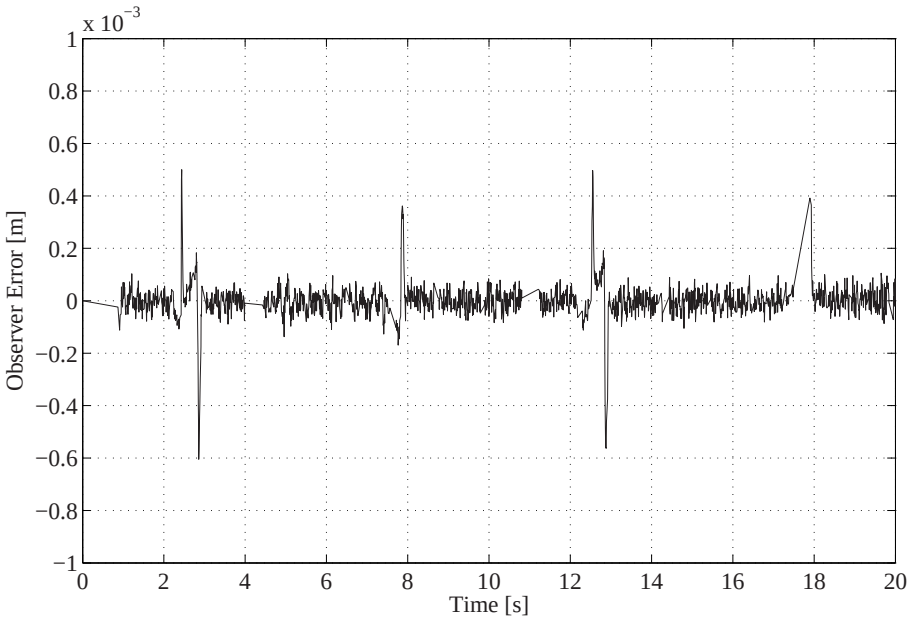

Figure 5.5: Experimental results for $y_{\mathrm{d}1}(t)$. Observer error z for the control algorithm of Section 3.3.

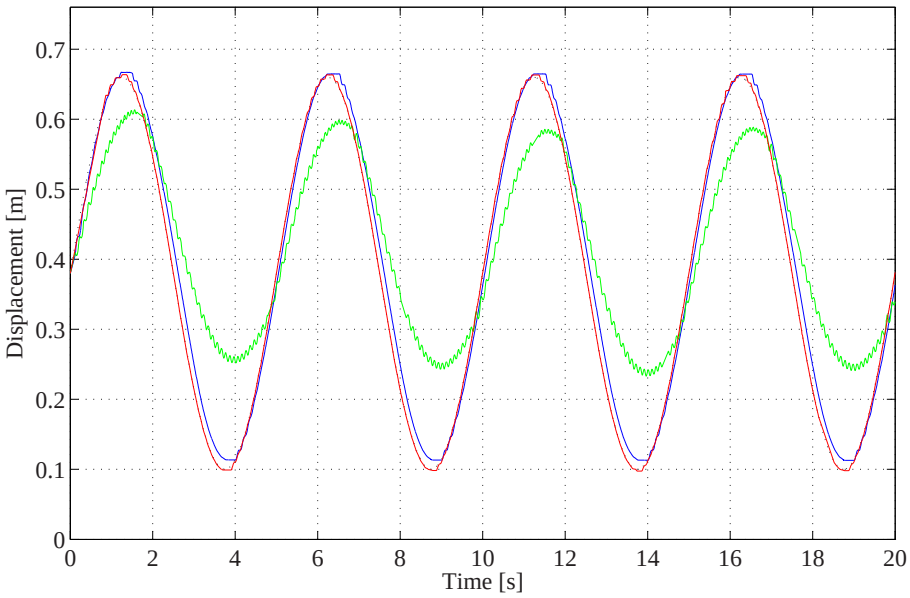

Figure 5.6: Experimental results for $y_{d2}(t)$. ($\cdots$) Desired trajectory. (——) PID Control. (——) Sliding mode control. (——) Control algorithm of Section 3.3.

5.2 Experimental results for $y_{d2}(t)$

This experiment is a sinus signal like the one for $y_{d1}(t)$ in (5.1), but twice faster. As shown in Figures 5.6 and 5.7, but specially in Table 5.4, the performance for the sliding mode control has decreased dramatically, while it got slightly worse for the both PID's, the regular one and the modified shown in Section 3.3. As before the input for the sliding mode controller has chattering (see Figure 5.8) and the pressures in both chambers remain under p_s in all cases (see Figure 5.9). We note that the better performance for the last scheme may be due to the implementation of an observer, as suggested by the experimental analysis presented in Arteaga-Pérez and Kelly (2004). In Figure 5.10 the corresponding observation error is shown.

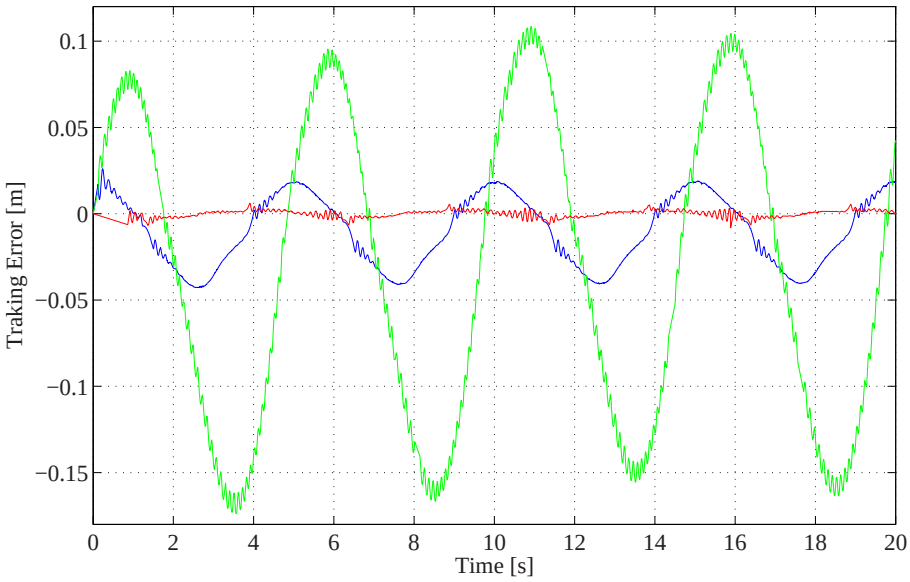

Figure 5.7: Experimental results for $y_{d2}(t)$. Tracking error Δy. (——) PID Control. (——) Sliding mode control. (——) Control algorithm of Section 3.3.

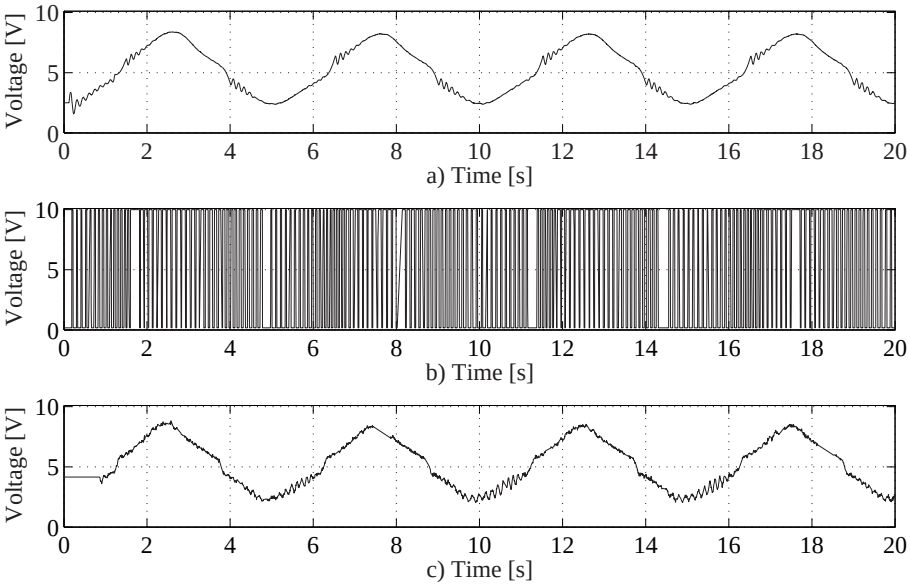

Figure 5.8: Experimental results for $y_{d2}(t)$. Input voltage u. a) PID Control. b) Sliding mode control. c) Control algorithm of Section 3.3.

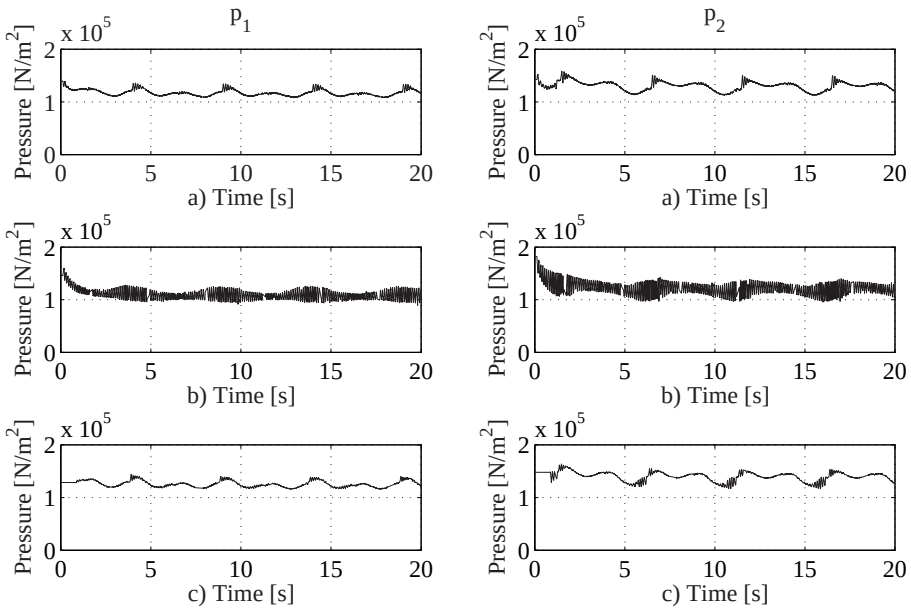

Figure 5.9: Experimental results for $y_{\mathrm{d}2}(t)$. Pressures in chambers 1 and 2. a) PID Control. b) Sliding mode control. c) Control algorithm of Section 3.3.

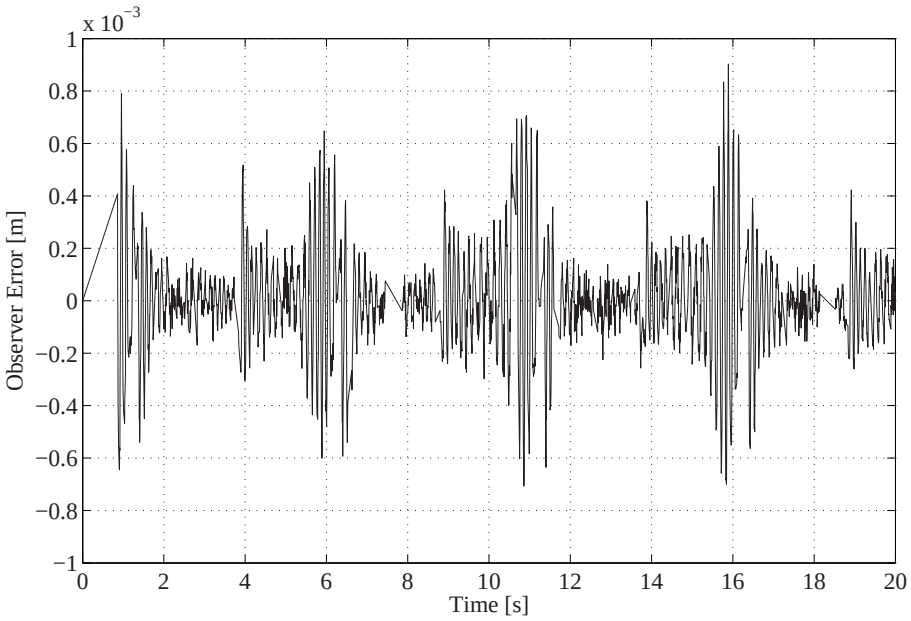

Figure 5.10: Experimental results for $y_{\mathrm{d}2}(t)$. Observer error z for the control algorithm of Section 3.3.

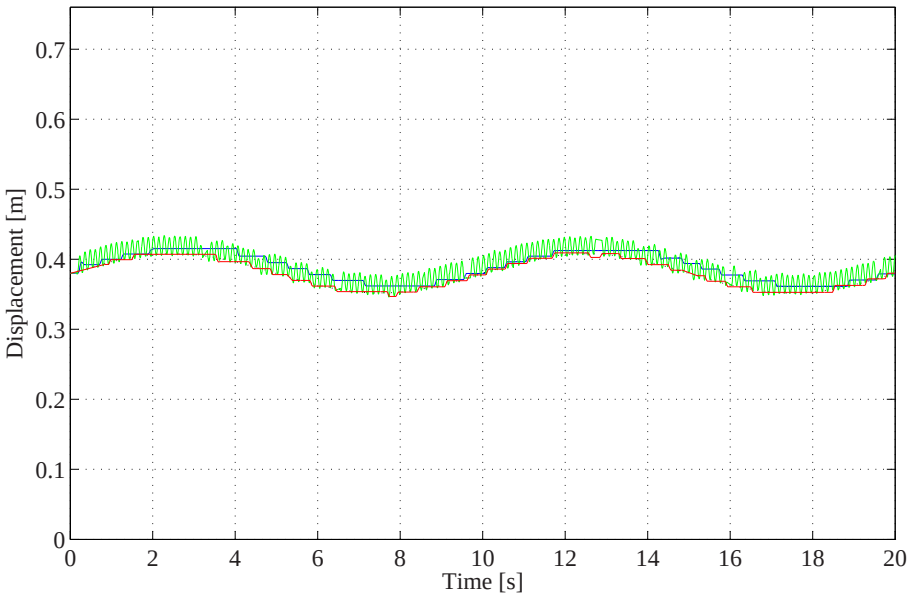

Figure 5.11: Experimental results for $y_{\mathrm{d}3}(t)$. ($\cdots$) Desired trajectory. (——) PID Control. (——) Sliding mode control. (——) Control algorithm of Section 3.3.

5.3 Experimental results for $y_{\mathrm{d}3}(t)$

The third experiment uses the same frequency as for $y_{\mathrm{d}1}(t)$ but is ten times slower, *i. e.* the magnitude is ten times smaller so that the movement is finer. Our aim is to try to show up some friction effects, like the Coulomb one. However, as can be seen in Figures 5.11 to 5.15 the outcomes are similar than those for the first case, although the PID performance clearly improves while the other two approaches became slightly worse (see Table 5.4). Note that this can either show a robust performance or a lack of strong friction effects at low velocities. There are no saturation in the chambers and certainly the sliding mode controller shows chattering again. The last two experiments will give rise to the conclusion that there may be in fact friction effects present but the slow movement somehow helps the PID (see Sections 5.5 and 5.6).

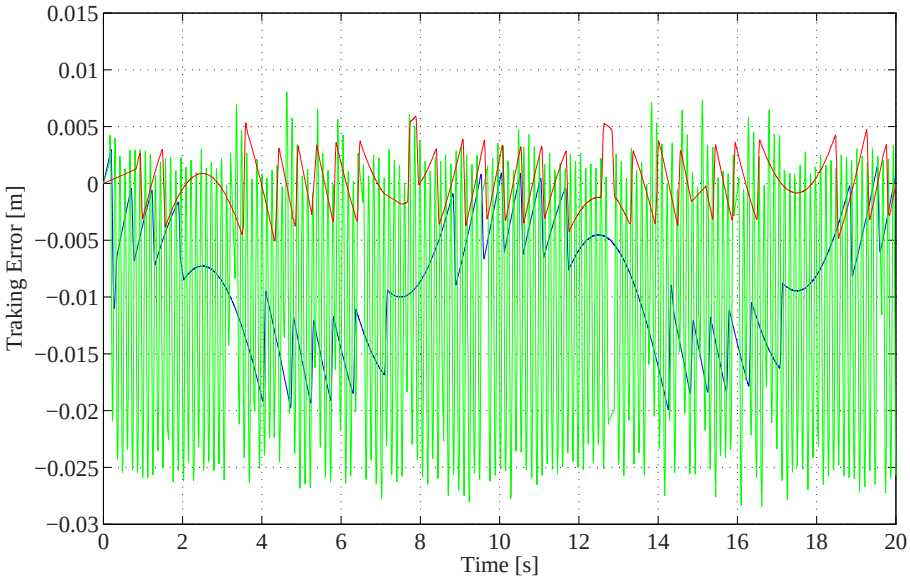

Figure 5.12: Experimental results for $y_{\mathrm{d}3}(t)$. Tracking error Δy. (——) PID Control. (——) Sliding mode control. (——) Control algorithm of Section 3.3.

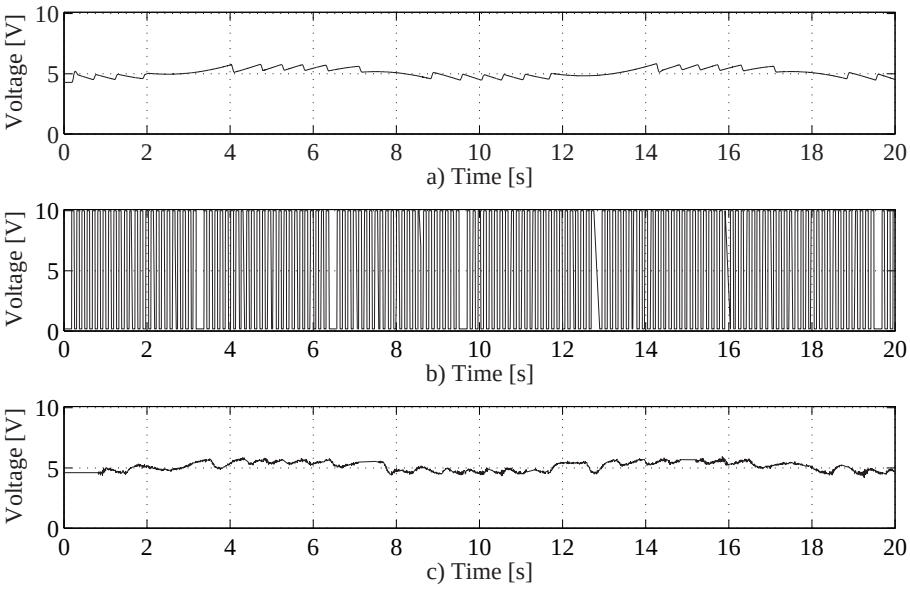

Figure 5.13: Experimental results for $y_{\mathrm{d}3}(t)$. Input voltage u. a) PID Control. b) Sliding mode control. c) Control algorithm of Section 3.3.

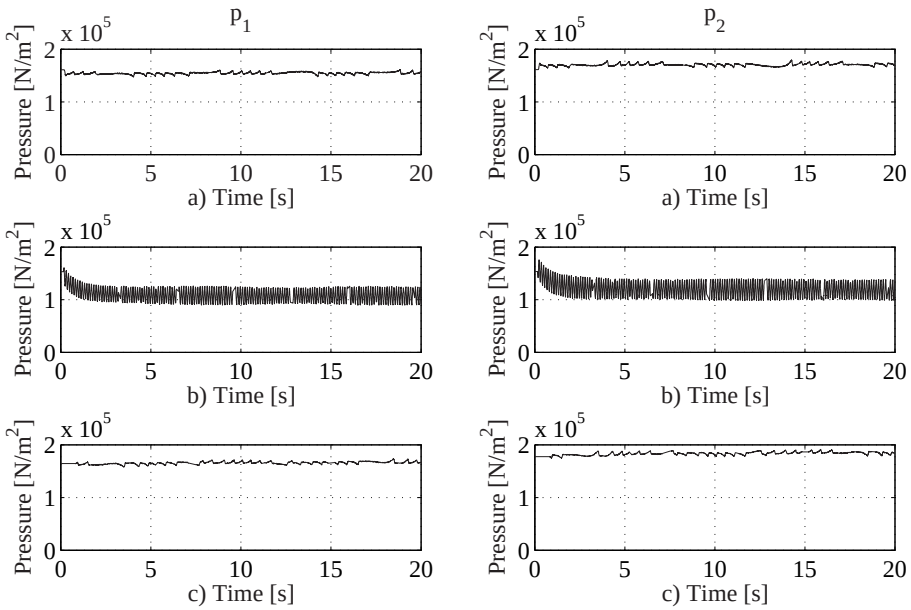

Figure 5.14: Experimental results for $y_{\mathrm{d}3}(t)$. Pressures in chambers 1 and 2. a) PID Control. b) Sliding mode control. c) Control algorithm of Section 3.3.

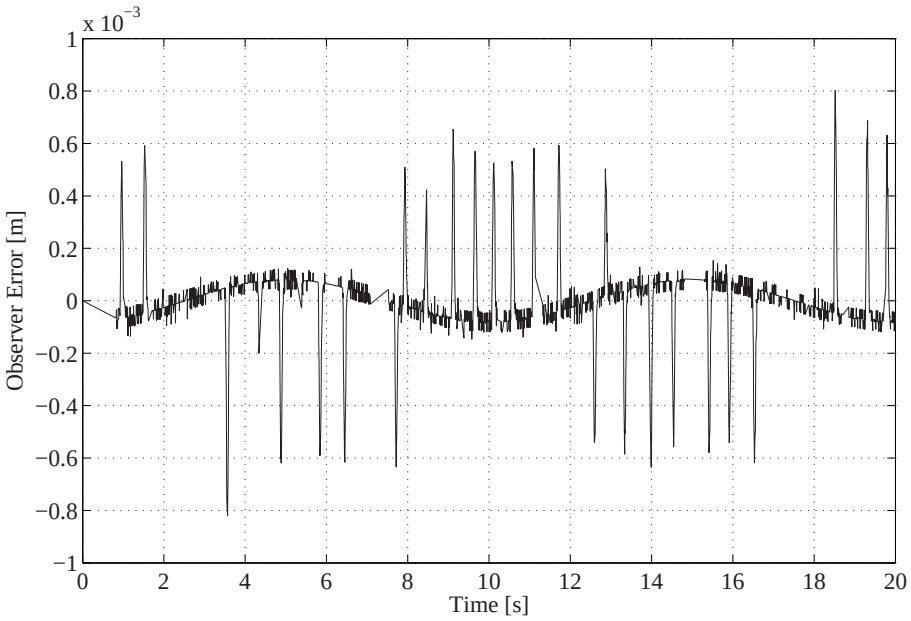

Figure 5.15: Experimental results for $y_{\mathrm{d}3}(t)$. Observer error z for the control algorithm of Section 3.3.

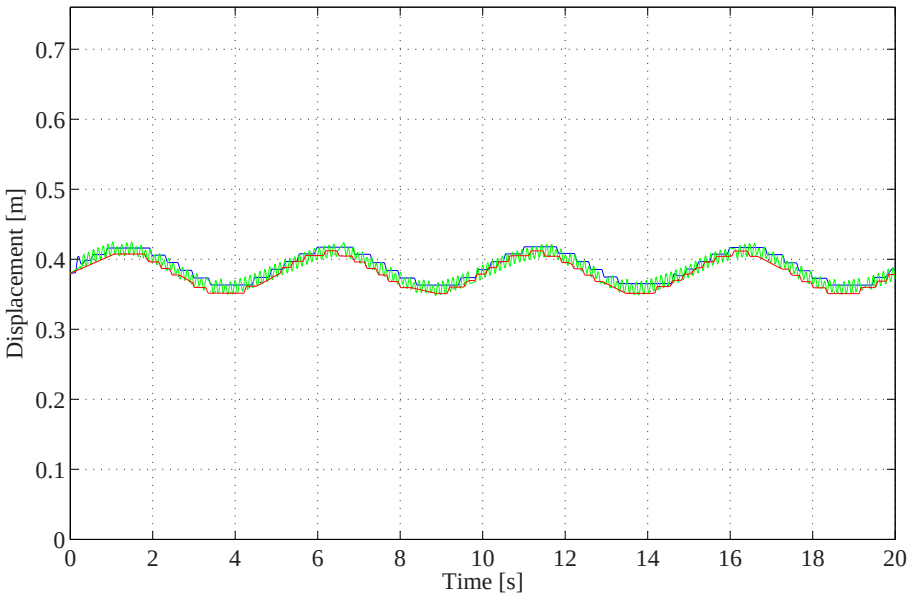

Figure 5.16: Experimental results for $y_{\mathrm{d}4}(t)$. $(\cdots)$ Desired trajectory. (——) PID Control. (——) Sliding mode control. (——) Control algorithm of Section 3.3.

5.4 Experimental results for $y_{\mathrm{d}4}(t)$

We try a frequency twice higher as that for the third experiment. As can be appreciated in Figures 5.16 to 5.19 the performance has increased again, except for the last approach where it remains pretty much the same (see Table 5.4). Therefore, for this fine movement we can conclude that the system response is more sensitive to a lower velocity, which might be associated to Coulomb friction. Finally, as may have been expected, the observation error tends to zero as before (see Figure 5.20).

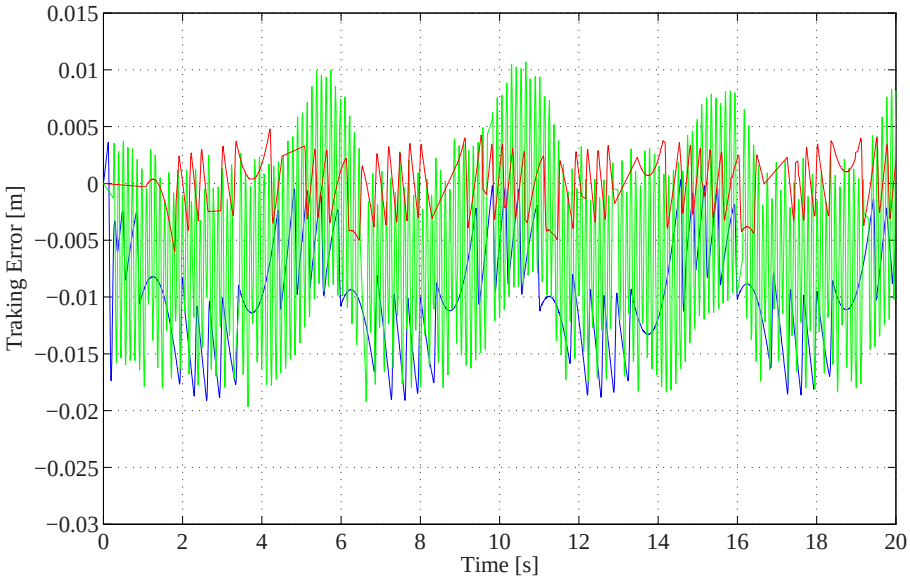

Figure 5.17: Experimental results for $y_{\mathrm{d}4}(t)$. Tracking error Δy. (——) PID Control. (——) Sliding mode control. (——) Control algorithm of Section 3.3.

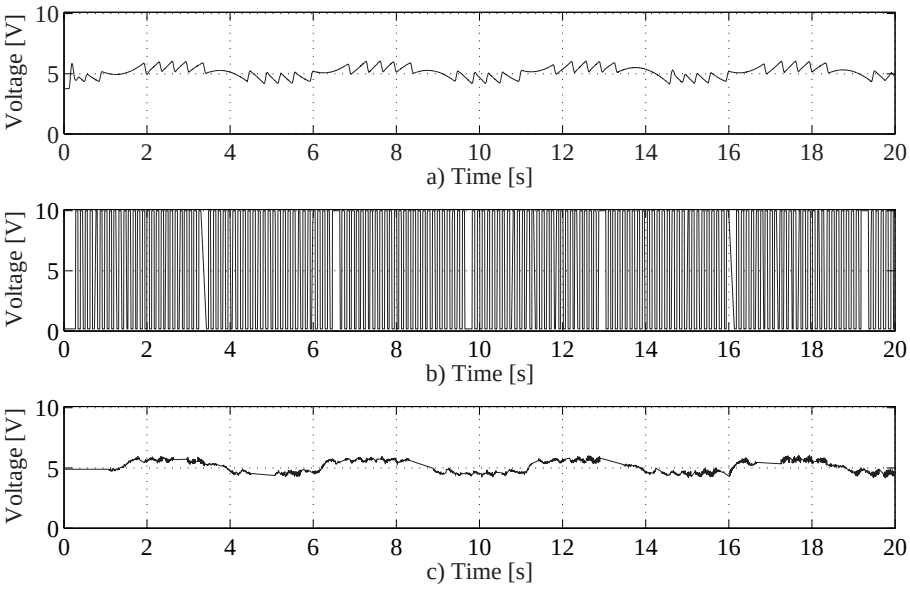

Figure 5.18: Experimental results for $y_{\mathrm{d}4}(t)$. Input voltage u. a) PID Control. b) Sliding mode control. c) Control algorithm of Section 3.3.

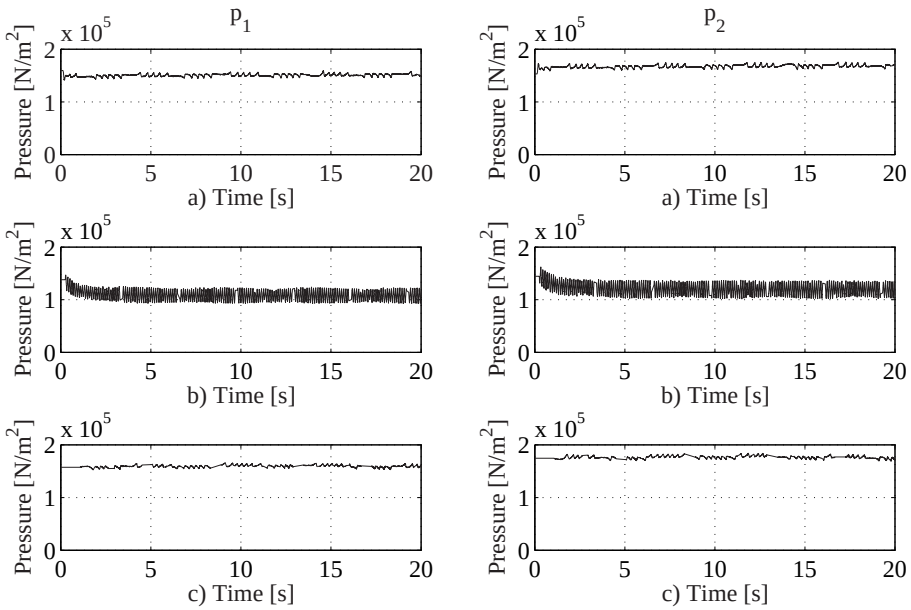

Figure 5.19: Experimental results for $y_{\mathrm{d}4}(t)$. Pressures in chambers 1 and 2. a) PID Control. b) Sliding mode control. c) Control algorithm of Section 3.3.

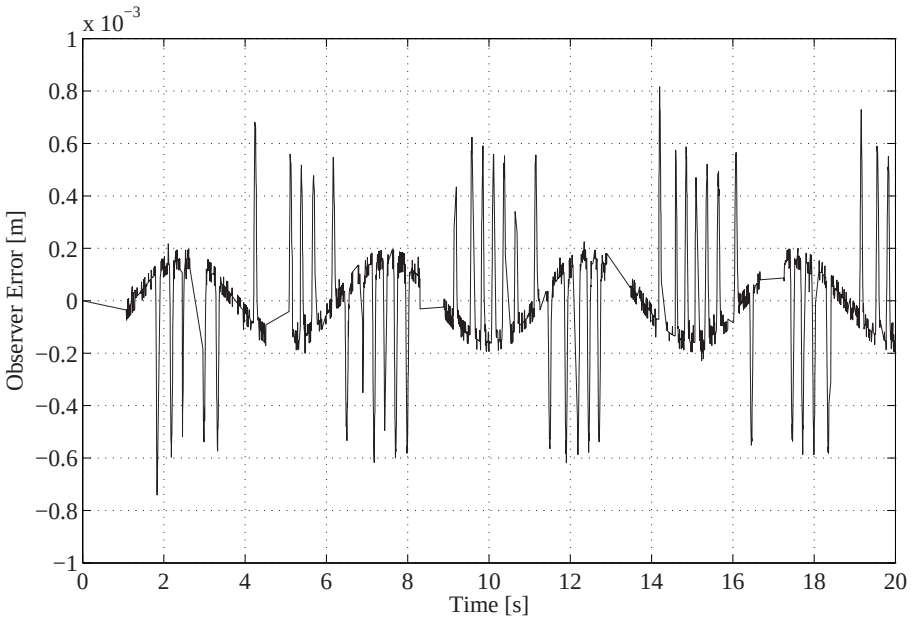

Figure 5.20: Experimental results for $y_{\mathrm{d}4}(t)$. Observer error z for the control algorithm of Section 3.3.

5.5 Experimental results for $y_{\mathrm{d}5}(t)$

As has been shown till now, fast movements demand a higher performance from the control laws. To test this under harder conditions we have chosen a square wave, rich in frequencies (see equation (5.5)). First of all we try to move the piston along almost the whole work space and in the last experiment only a small amplitude for the square wave will be employed. By choosing $y(0) = 0.1\mathrm{m}$ the desired trajectory allows to appreciate the step response of the system as well. In Figures 5.21 and 5.22 can be seen that the PID is not able to eliminate the residual error. Since an integral term has been included, this may be due to the presence of non modeled effects, like Coulomb friction. Note that the sliding mode algorithm does not reach the final value because it cannot make the system respond fast enough, while the algorithm of Section 3.3 can eliminate the residual error by responding faster. This is not at the cost of producing chattering, although the required wide movement causes saturation for some time. This means that the zero error cannot be gotten faster (see Figure 5.23). Despite this the supply pressure is not reached in any chamber, as can be appreciated in Figure 5.24. Of course, in Table 5.4 the RMSE index is very high in each case because the error becomes large for every change in the wave form. Finally, in Figure 5.25 can be seen that the observation error tends to zero as well. Note that the abrupt change due to the square wave causes the error to increase every 2.5s.

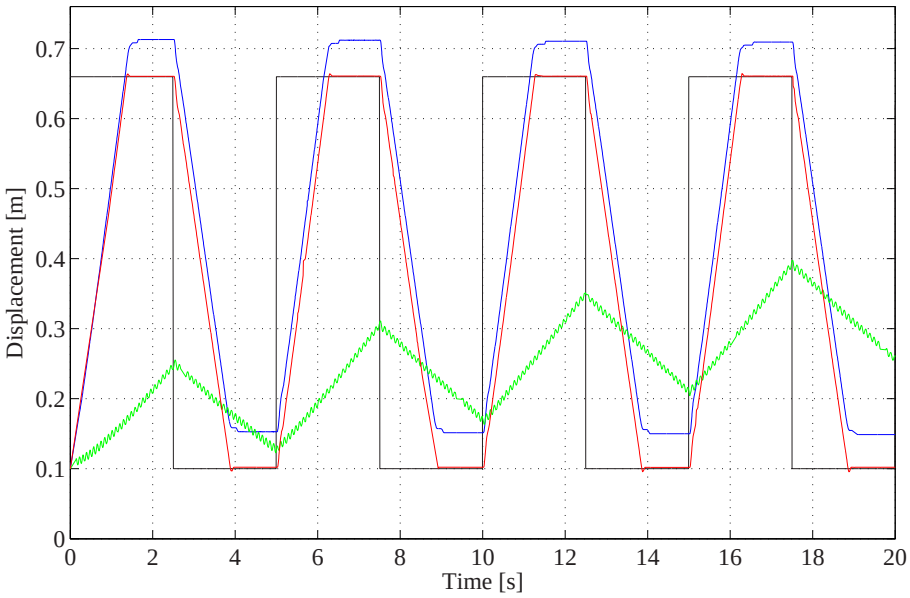

Figure 5.21: Experimental results for $y_{\mathrm{d}5}(t)$. (——) Desired trajectory. (——) PID Control. (——) Sliding mode control. (——) Control algorithm of Section 3.3.

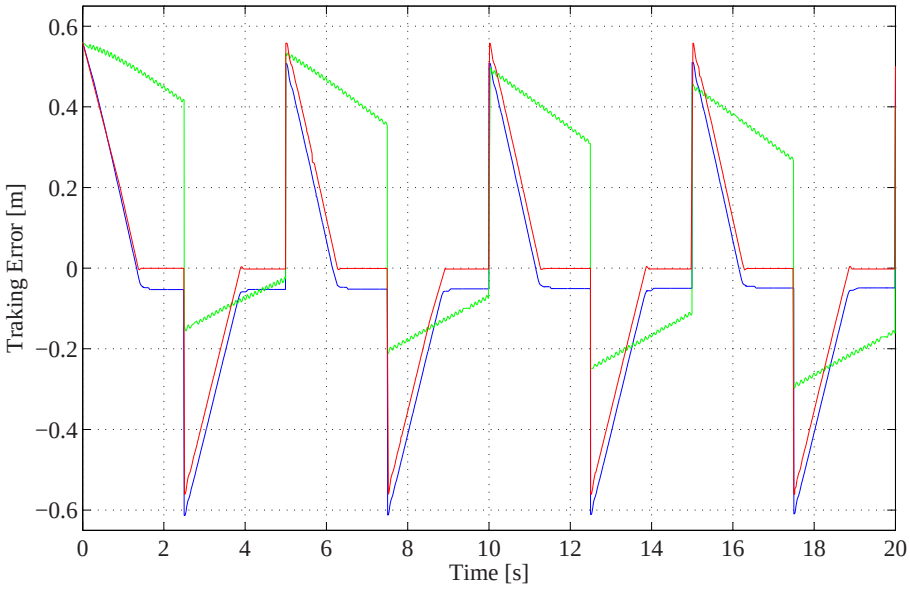

Figure 5.22: Experimental results for $y_{\mathrm{d}5}(t)$. Tracking error Δy. (——) PID Control. (——) Sliding mode control. (——) Control algorithm of Section 3.3.

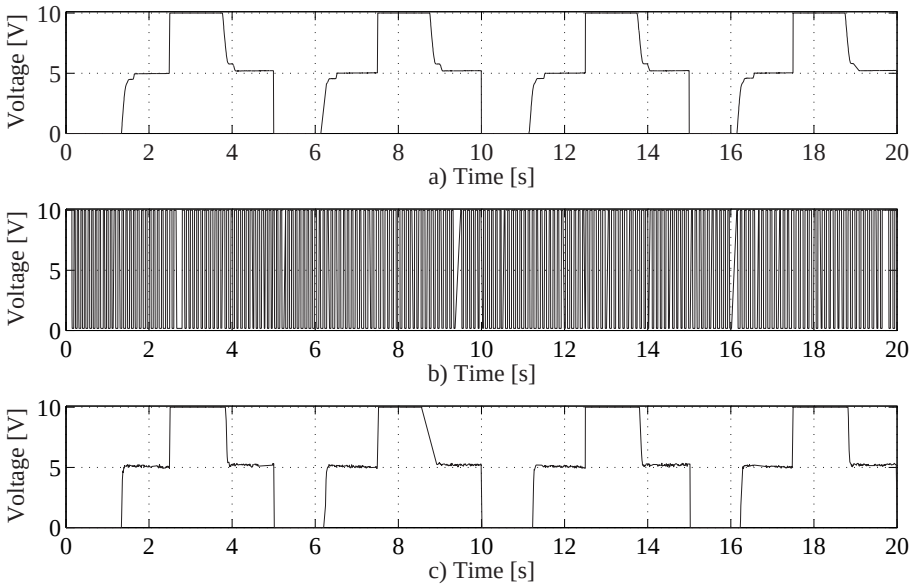

Figure 5.23: Experimental results for $y_{\mathrm{d}5}(t)$. Input voltage u. a) PID Control. b) Sliding mode control. c) Control algorithm of Section 3.3.

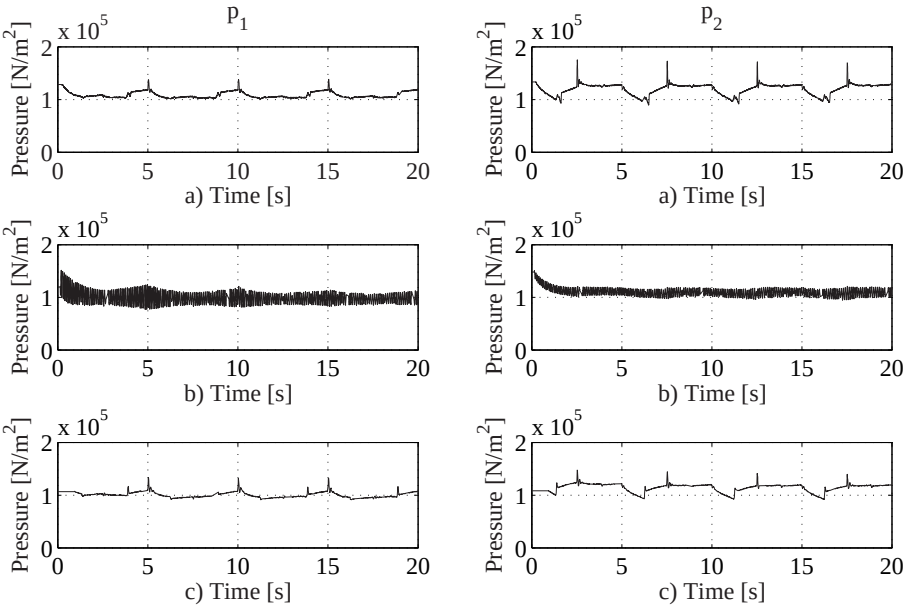

Figure 5.24: Experimental results for $y_{\mathrm{d}5}(t)$. Pressures in chambers 1 and 2. a) PID Control. b) Sliding mode control. c) Control algorithm of Section 3.3.

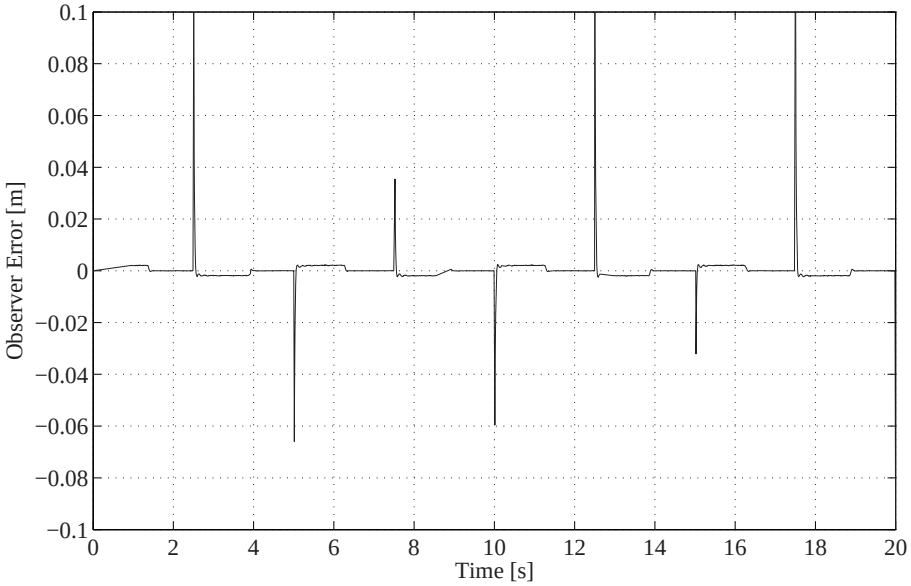

Figure 5.25: Experimental results for $y_{\mathrm{d}5}(t)$. Observer error z for the control algorithm of Section 3.3.

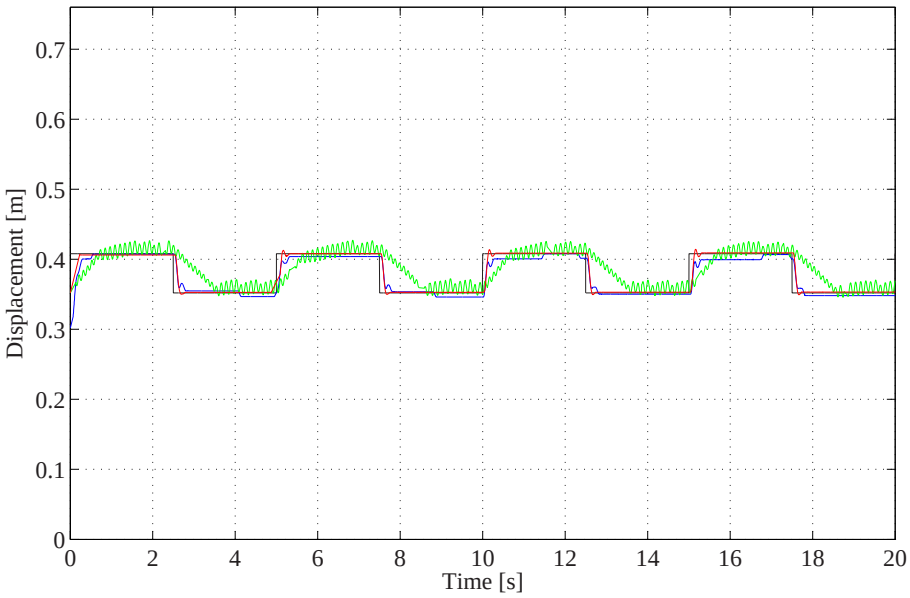

Figure 5.26: Experimental results for $y_{\mathrm{d}6}(t)$. (——) Desired trajectory. (——) PID Control. (——) Sliding mode control. (——) Control algorithm of Section 3.3.

5.6 Experimental results for $y_{\mathrm{d}6}(t)$

The last experiment uses the square wave again but with only a narrow movement. As before, the PID cannot achieve the zero error, which appears to confirm the presence of Coulomb friction. Also, the sliding mode control cannot eliminate the residual error and it shows chattering as before. On the other hand, the algorithm of Section 3.3 is able to follow the desired trajectory very accurately. This cannot be fully appreciated in Table 5.4 because the error increases every 2.5s. See Figures Figure 5.26 to 5.28. As usual the pressures in the chambers do not reach the supply pressure $\mathrm{p_s}$ in any case (see Figure 5.29) and the observation error becomes zero when the observer is employed (see Figure 5.30).

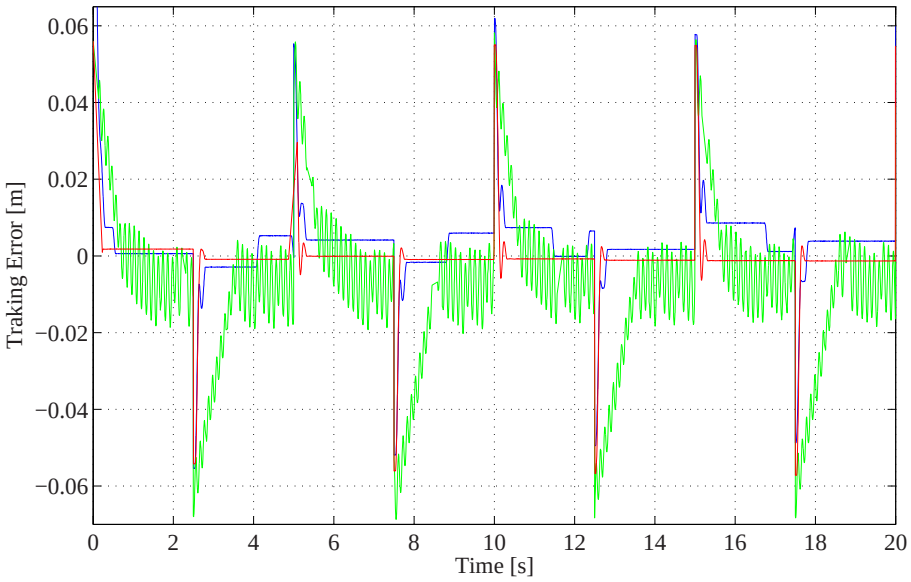

Figure 5.27: Experimental results for $y_{\mathrm{d}6}(t)$. Tracking error Δy. (——) PID Control. (——) Sliding mode control. (——) Control algorithm of Section 3.3.

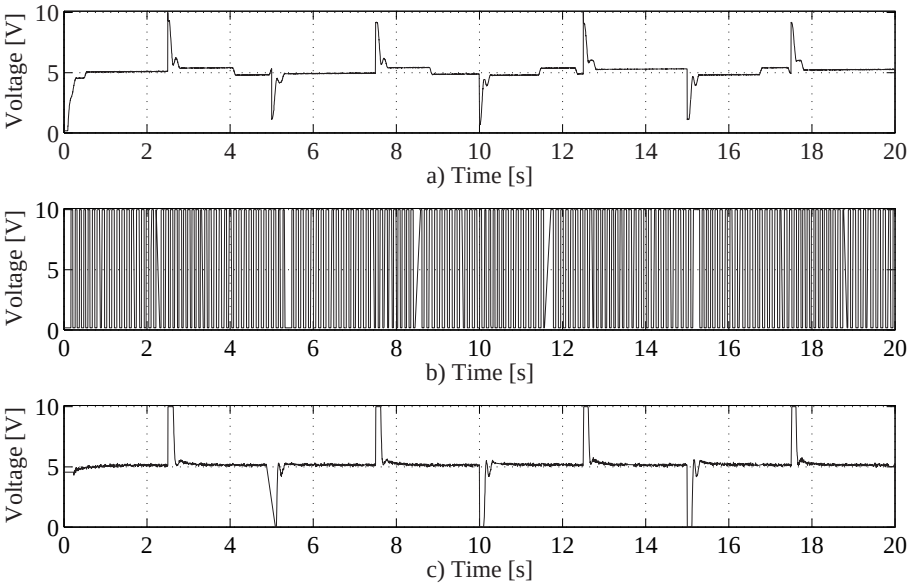

Figure 5.28: Experimental results for $y_{\mathrm{d}6}(t)$. Input voltage u. a) PID Control. b) Sliding mode control. c) Control algorithm of Section 3.3.

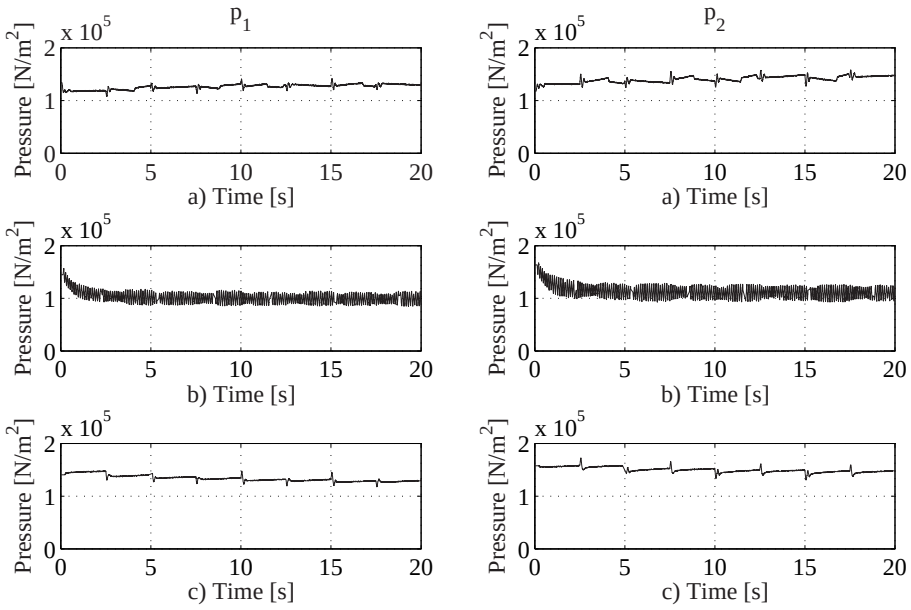

Figure 5.29: Experimental results for $y_{\mathrm{d}6}(t)$. Pressures in chambers 1 and 2. a) PID Control. b) Sliding mode control. c) Control algorithm of Section 3.3.

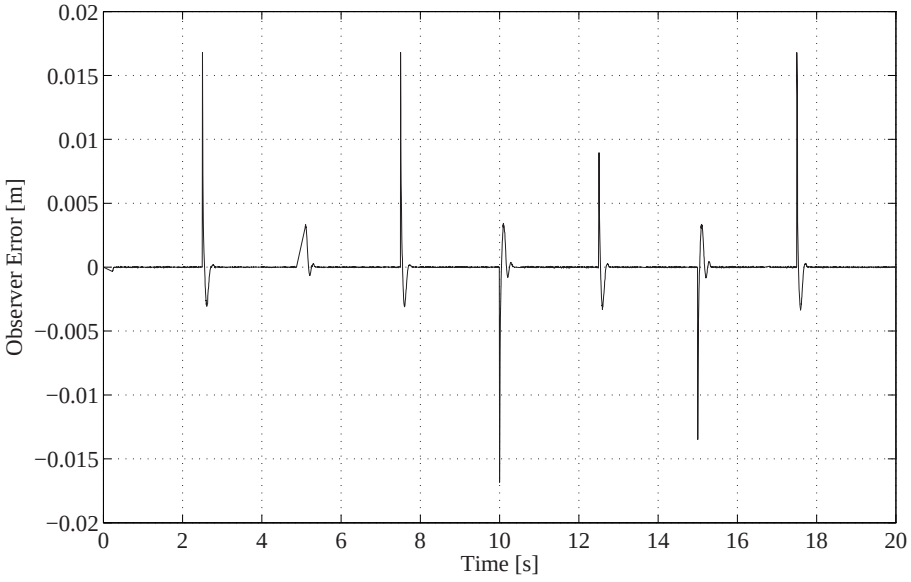

Figure 5.30: Experimental results for $y_{\mathrm{d}6}(t)$. Observer error z for the control algorithm of Section 3.3.

5.7 Discussion

After analyzing the different experiments, we conclude that a simple PID should always be the first option if no high performance is required. This is because of its simplicity and the acceptable results obtained altogether. Furthermore, for a system with less friction a better step response and nearly zero residual error should be expected. If the performance has to be increased sliding mode techniques represent a good alternative. However, we note that a first order sliding mode control has the well–known disadvantage of chattering and a relative slow response. Also, the approach used in this work requieres a rough linear model for implementation. Since the results obtained are rather bad, we conclude that for such a complex system a linear model could have been expected not to be good enough. Also, computing proper parameters as we have done was very straightforward but maybe the dynamic description could still be improved. This, however, is what we tried to avoid for our comparison analysis. Finally, the last algorithm represents a combination of PID with sliding mode, which clearly allows to improve system performance. We note that estimating the piston velocity with an observer instead of numerical differentiation also provides smother results but this is not necessary for stability purposes. For implementation of this approach the cross section areas of piston chambers are required, what represents (static) information of the system that can be known accurately. A force sensor could avoid this requirement. Therefore, we can claim that the control–observer scheme in Section 3.3 can be implemented rather easily with no dynamic model information, thus representing a very good alternative to regular PID's.

Finally, to get a more objective insight of the results the Root Mean Square Error (RMSE) suggested in Ning and Bone (2005) has been computed as

$$\text{RMSE} = \sqrt{\frac{1}{n}\sum_{i=1}^{n} e_i^2}, \tag{5.7}$$

where i the current sample number , e_i the error associated to i and n the total number of samples. The results in [mm] are shown in Table 5.4, showing the algorithm of Section 3.3 has the best performance.

Trajectory	PID	Sliding mode control	Algorithm of Section 3.3
y_{d1}	19.369	13.756	1.435
y_{d2}	22.259	94.943	2.139
y_{d3}	10.343	14.619	2.227
y_{d4}	7.098	8.893	2.252
y_{d5}	245.301	327.969	223.702
y_{d6}	10.449	22.126	8.887

Table 5.4: Root mean square errors in [mm].

Chapter 6

Conclusions and contributions

6.1 Conclusions

In this thesis, modeling of differential pneumatic pistons with proportional valves was discussed and it was shown that getting an accurate model to describe the system dynamics represents a demanding challenge and a need of high power CPU's. Although parameter estimation algorithms can be employed to get a good mathematical representation for this kind of devices, it was shown that for control purposes only a rough approximation or no model at all can be enough. In doing so, some common approaches like feedback linearization have been excluded from this work, while a dynamic model is employed only for studying physical properties.

Three control schemes are implemented into the experimental system and tested to determine their performance: a regular PID because it is still the most employed in industry, a sliding mode control law available in the literature which uses a rough linear model of the system for implementation and a modified PID algorithm designed originally for robot manipulators. The last one uses a sign function in the integral term, to get a smoother control without chattering, and a velocity observer to avoid numerical differentiation. The experimental results show that for low performance a regular PID is enough, but for higher performance sliding mode techniques are a good alternative. The modified algorithm clearly shows the best performance with no chattering.

An observability analysis is also done, but as a lack of time not used in this work. The main conclusion of this part is that the system is observable if displacement y and pressures p_1 or p_2 are available.

In view of the outcomes, as future work it should be considered the implementation of other control techniques which have proven to be effective for high nonlinear systems and which do not required model information. In particular, Generalized Proportional Integral (GPI) controllers and observers should

be tested because this is a linear technique that naturally compensates the unknown system dynamics and perturbations, thus improving performance. Also, if possible the control algorithms should be tested in an industrial environment to get an even better insight of the performance of each scheme in an real environment and nearly real task.

6.2 Contributions

The first steps of the investigation on this subject, including the first simulated comparison of different control laws were published as Weist and Arteaga (2009). This paper contains the conclusion, that model free control laws and even model based control laws have advantages over simple control laws as PID's *e. g.*.

- Authors: Weist, J., and Arteaga–Pérez, M.A.
- Title: Comparison of different control algorithms for pneumatic actuators
- Published in: *Proceedings CD-ROM Congreso Anual de la Asociación de México de Control Automático (AMCA). Zacatecas, México*
- Date: 30th September to 2th October 2009

In Weist *et al.* (2011) the part of the adapting of the control law proposed in this tesis and an experimental comparison was published. The experimental comparison includes three different non model based control laws.

- Authors: Weist, J., Arteaga–Pérez, M.A., de la Cruz, L., and Hebisch, H.
- Title: Model free control for differential pneumatic pistons: experimental comparison
- Published in: *International Journal of Control*
- Volume: 84
- Number: 1
- Pages: 138-164
- Date: January 2011

Appendix A – Experimental test bed and model validation

For the experimental comparison of different control laws the test-bed shown in Figure A.1 has been employed. This is a *Telemecanique* actuator provided with a *Festo* proportional valve MYPE–5–1/8–HF–010 B, a *Festo* pressure sensor for each piston–chamber and the air supply, as well as a *Sick–Stegmann* absolute encoder for reading the piston position. It is controlled with a *CompactRio* acquisition system by *National Instruments* with a programmed sampling time of 1.5ms. The air is distributed by an 230 liters air compressor *Craftsman Professional* and a *Festo* maintenance system with regulator. By disconnecting the different parts of the pneumatic system, the following data has been obtained: $A_1 = 5.0265 \cdot 10^{-4}\text{m}^2$, $A_2 = 4.5357 \cdot 10^{-4}\text{m}^2$, $M = 5.8\text{kg}$, $V_{10} = 1.5 \cdot 10^{-5}\text{m}^3$, $V_{20} = 1.35 \cdot 10^{-5}\text{m}^3$, $L = 0.76\text{m}$, $L_1 = 0.03\text{m}$ and, $L_2 = 0.03\text{m}$. Also it was calculated that $F_\text{V} \approx 240\,(\text{N}\cdot\text{m})/\text{s}$, and it is used $\gamma = 1.4$, $R = 287.05\,\text{J}/(\text{kg}\cdot\text{K})$, $T = 293.15\text{K}$, $\rho_0 = 1.204\,\text{kg}/m^3$ and $b = 0.582$ from DIN 1306 (1984), DIN 1343 (1990) and ISO 6358 (1989). Furthermore, it is assumed $C(u) = 0.8u$.

To validate the model, the output y is compared with simulation results implemented in *SimuLink*. We have employed the following test signals:

$$u_1(t) = 5\sin(1.0 \cdot 2\pi t) + 5 \quad [\text{V}] \tag{A.1}$$
$$u_2(t) = 5\sin(0.5 \cdot 2\pi t) + 5 \quad [\text{V}] \tag{A.2}$$
$$u_3(t) = 5\sin(0.1 \cdot 2\pi t) + 5 \quad [\text{V}] \tag{A.3}$$
$$u_4(t) = 5\,\text{square}(1.0 \cdot 2\pi t) + 5 \quad [\text{V}] \tag{A.4}$$
$$u_5(t) = 5\,\text{square}(0.5 \cdot 2\pi t) + 5 \quad [\text{V}] \tag{A.5}$$
$$u_6(t) = 5\,\text{square}(0.1 \cdot 2\pi t) + 5 \quad [\text{V}] \tag{A.6}$$

The results for the test signals u_1, u_2, u_3, u_4, u_5 and u_6 are shown respectively in Figures A.2, A.3, A.4, A.5, A.6 and A.7. Clearly, the outcomes are not exact although length and masses were measured accurately. Certainly, the model could be improved by carrying out parameter estimation or by introducing other terms, like dynamic friction. However, for control purposes we claim that it is

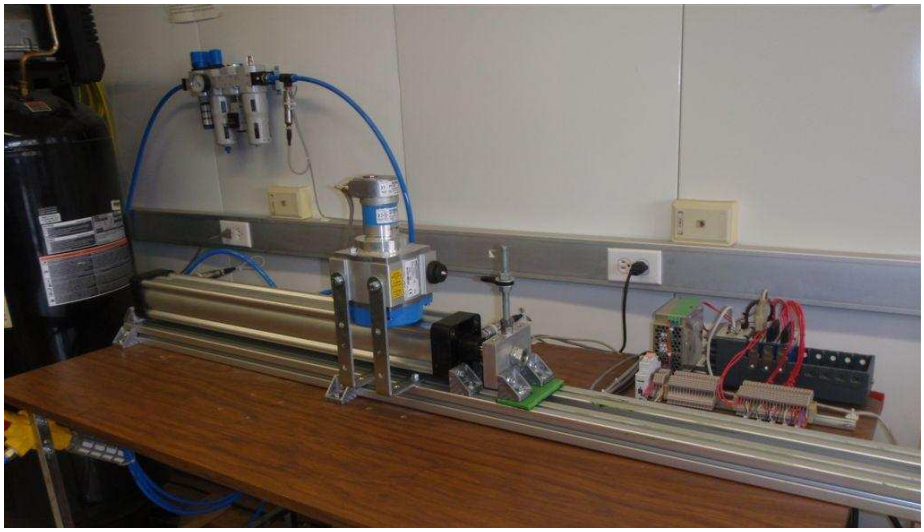

Figure A.1: Experimental test bed

much better to employed robust techniques.

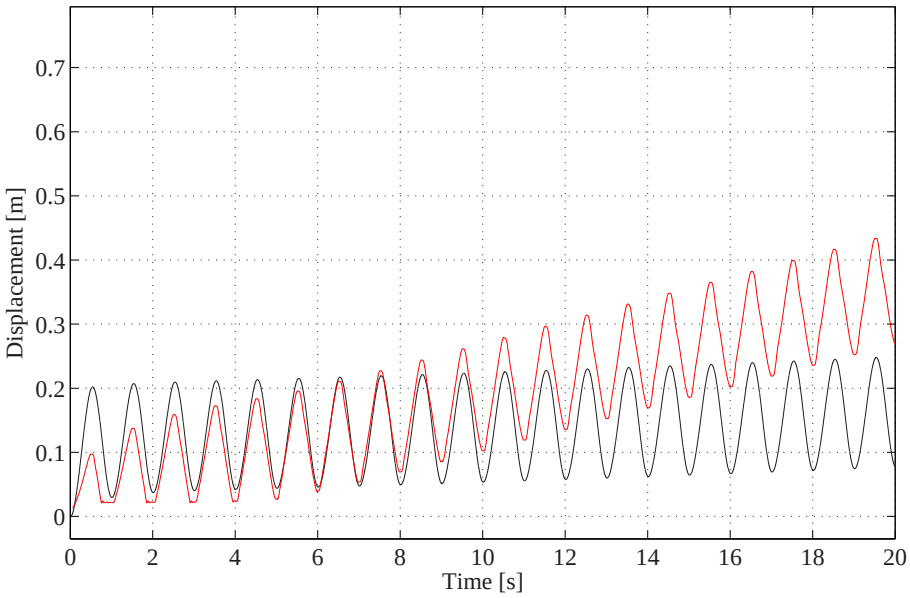

Figure A.2: Simulation results for test signal $u_1(t)$. (——) Displacement y *SimuLink*. (——) Displacement y Experimental System

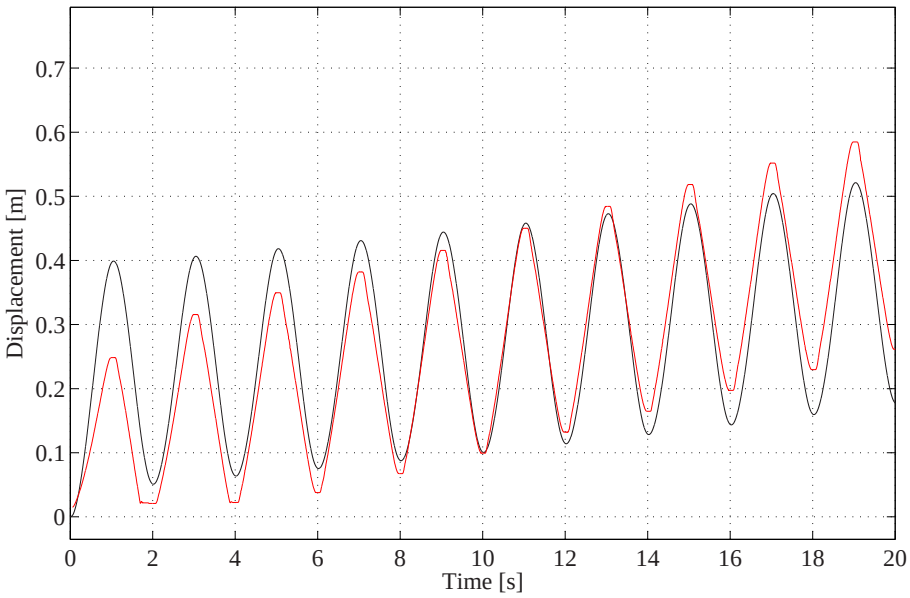

Figure A.3: Simulation results for test signal $u_2(t)$. (——) Displacement y *SimuLink*. (——) Displacement y Experimental System

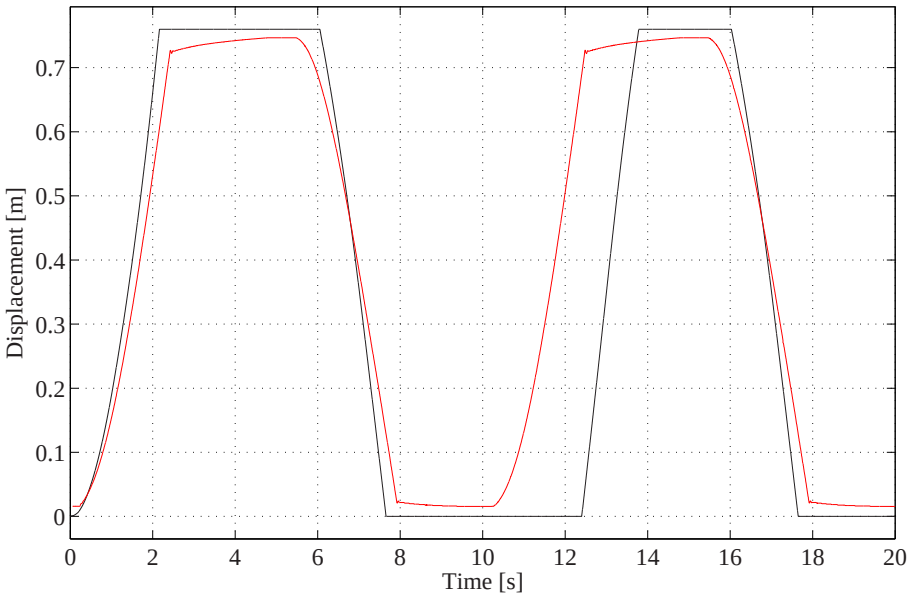

Figure A.4: Simulation results for test signal $u_3(t)$. (——) Displacement y *SimuLink*. (——) Displacement y Experimental System

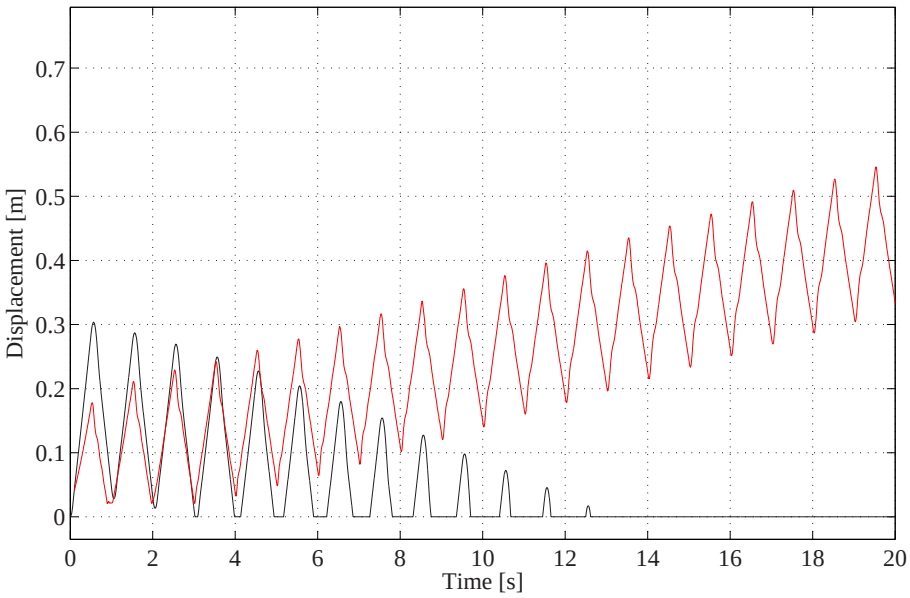

Figure A.5: Simulation results for test signal $u_4(t)$. (——) Displacement y *SimuLink*. (——) Displacement y Experimental System

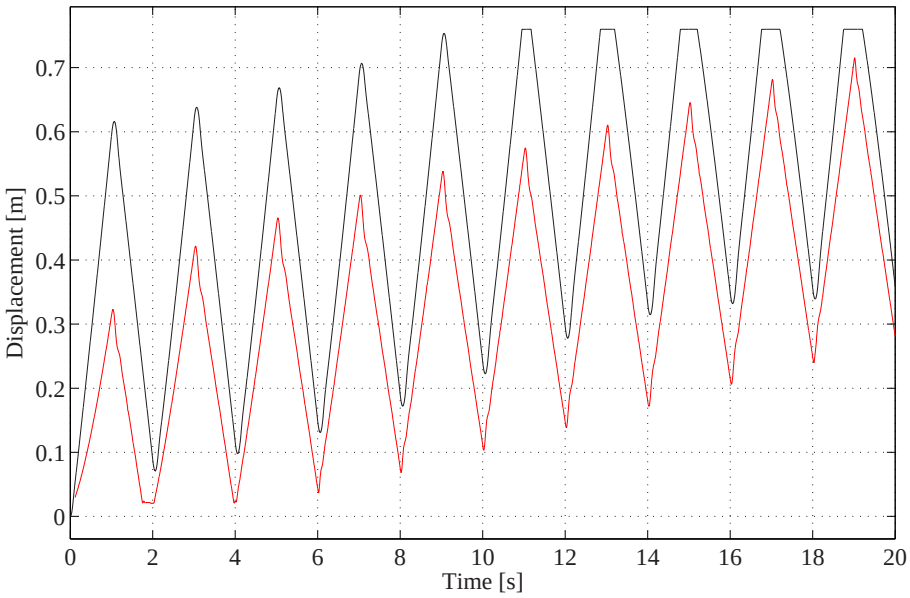

Figure A.6: Simulation results for test signal $u_5(t)$. (——) Displacement y *SimuLink*. (——) Displacement y Experimental System

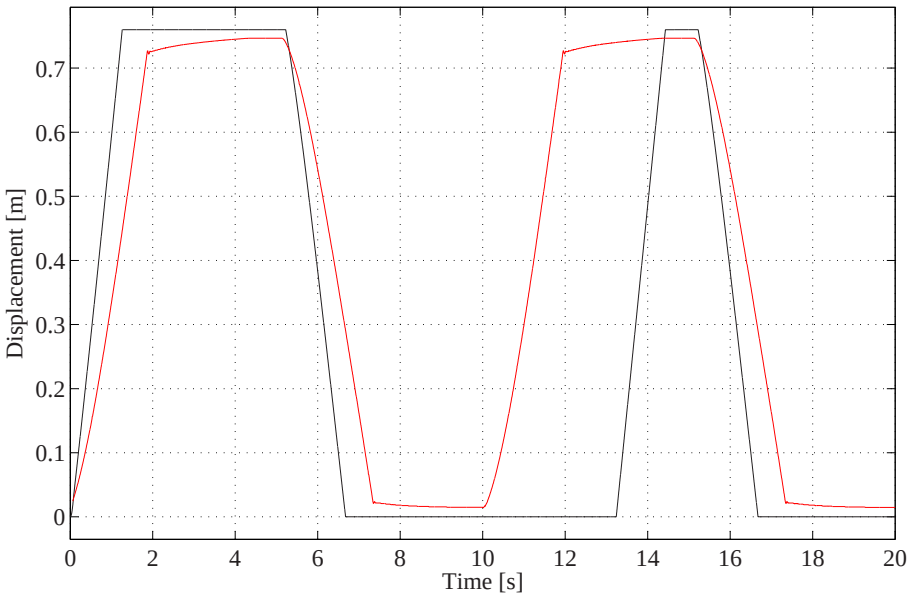

Figure A.7: Simulation results for test signal $u_6(t)$. (——) Displacement y *SimuLink*. (——) Displacement y Experimental System

Appendix B – Proof of Theorem 1

The algorithm of Chapter 3 is a direct adaptation of the control–observer scheme presented in Arteaga-Pérez *et al.* (2006) for robot manipulators. Thus, the proof is essentially the same and we will try to keep it as short as possible. For the reader interested in details it is highly advisable to have the references available. First of all, we summarized the main result of the reference in the following theorem.

Theorem 1 *Arteaga-Pérez et al. (2006)*
Consider

$$\boldsymbol{\sigma}(\boldsymbol{s}) = \int_0^t (\boldsymbol{K}_\beta \boldsymbol{s} + \operatorname{sign}(\boldsymbol{s}))\, \mathrm{d}\vartheta \qquad\qquad \boldsymbol{\sigma}(\mathbf{0}) = \mathbf{0} \tag{B.1}$$

where $\boldsymbol{\sigma}, \boldsymbol{s} \in \mathbb{R}^n$ *and* $\boldsymbol{K}_\beta \in \mathbb{R}^{\mathrm{n\,x\,n}}$ *is a diagonal positive definite matrix. Suppose that the following relationship*

$$\boldsymbol{e} = \boldsymbol{s} + \boldsymbol{K}_\gamma \boldsymbol{\sigma}(\boldsymbol{s}) \tag{B.2}$$

holds with $\boldsymbol{e} \in \mathbb{R}^n$ *bounded. If* $\boldsymbol{K}_\gamma \in \mathbb{R}^{\mathrm{n\,x\,n}}$ *is a diagonal positive definite matrix, then* $\boldsymbol{s}$, $\boldsymbol{\sigma}$ *and* $\dot{\boldsymbol{\sigma}}$ *are bounded as well. Additionally, if* $\dot{\boldsymbol{e}}$ *is bounded by* $\|\dot{\boldsymbol{e}}\| \leq e_{\max}$ *and if*

$$\phi \triangleq \lambda_{\min}(\boldsymbol{K}_\gamma) - e_{\max} > 0, \tag{B.3}$$

then $\boldsymbol{s} = \mathbf{0}$ *in a finite time satisfying* $t_{\mathrm{r}} \leq \frac{\|\boldsymbol{s}(\mathbf{0})\|}{\phi}$. △

The key point to employ Theorem 1 is to create equations of the form given by (B.1)–(B.2). As can be recognized, $\boldsymbol{s}$ represents a sliding variable whose tending to zero forces different system errors to tend to zero as well. To do the sketch of the proof we itemize it in the following steps.

a) A proper definition of the state of the closed loop dynamic for the algorithm of Section 3.3 is the following

$$s_{\mathrm{r}} \triangleq \dot{y} - \dot{y}_{\mathrm{r}} \tag{B.4}$$

$$r \triangleq \dot{y} - \dot{y}_{\mathrm{o}} = \dot{z} + \lambda_{\mathrm{z}} z \tag{B.5}$$

where $\dot{y}_{\mathrm{r}}$ is given in (3.15) and $\dot{y}_{\mathrm{o}}$ in (3.16). Also, by taking into account (3.23) the complete state is considered to be

$$\boldsymbol{\omega} = \begin{bmatrix} s_{\mathrm{r}} \\ s_{\mathrm{f}} \\ r \end{bmatrix}. \tag{B.6}$$

b) We show now the equations of the form (B.1)–(B.2) involved in our analysis and the relationship with the state $\boldsymbol{\omega}$. In fact, directly from equations (3.11) to (3.15) and (B.4) it is possible to get

$$\begin{aligned} s_{\mathrm{r}} &= \dot{y} - \dot{y}_{\mathrm{d}} + \lambda_{\mathrm{y}}\bar{y} - s_{\mathrm{d}} + k_{\gamma\mathrm{y}}\sigma_{\mathrm{y}} && \text{(B.7)} \\ &= \dot{z} + s_{\mathrm{y1}} + k_{\gamma\mathrm{y}}\sigma_{\mathrm{y}} \\ \Rightarrow \quad s_{\mathrm{y1}} + k_{\gamma\mathrm{y}}\sigma_{\mathrm{y}} &= s_{\mathrm{r}} - \dot{z}. && \text{(B.8)} \end{aligned}$$

To use Theorem 1 one just has to set $e = s_{\mathrm{r}} - \dot{z}$ and $s = s_{\mathrm{y1}}$. Should the state be bounded, then e will be so as well because the boundednees of r in (B.5) implies that of $\dot{z}$ and z. The involved variables s_{y1}, σ_{y} and $\dot{\sigma}_{\mathrm{y}}$ will be bounded too.

The other variable suitable to employ Theorem 1 is simply s_{f} in (3.23) with $e = s_{\mathrm{f}}$ and $s = \Delta x_{\mathrm{f}}$. Quite directly the boundedness of the state $\boldsymbol{\omega}$ guarantees that of Δx_{f}, σ_{f} and $\dot{\sigma}_{\mathrm{f}}$.

c) After Theorem 1, if $\dot{\boldsymbol{\omega}}$ is bounded then both s_{y1} and Δx_{f} will be zero in a finite time. While the later does not need any further analysis, the former has to be developed. In fact, from (3.11) to (3.13) one gets

$$s_{\mathrm{y}} = \dot{\bar{y}} + \lambda_{\mathrm{y}}\bar{y} = s_{\mathrm{y1}} + s_{\mathrm{d}} \qquad \text{bounded.} \tag{B.9}$$

Since this equation represents a stable linear filter for $\bar{y}$ with bounded input, then so the outputs will be $\bar{y}, \dot{\bar{y}}$. But since $\bar{y} = \hat{y} - y_{\mathrm{d}}$ and y_{d} and its derivatives are bounded by assumption then $\hat{y}$ and $\dot{\hat{y}}$ will be bounded as well. But, if in addition s_{y1} vanishes then both $\bar{y}$ and $\dot{\bar{y}}$ will tend to zero as well. As fully explained in Arteaga-Pérez *et al.* (2006), this implies that the tracking errors Δy and $\Delta\dot{y}$ as given in (3.19), as well as the observation errors z and $\dot{z}$ in (3.9) will tend to zero.

d) According to items b) and c) if the closed loop state $\boldsymbol{\omega}$ and its derivative are bounded, then all tracking and observation errors will tend to zero. Computing the closed loop dynamics is rather direct. By taking into account (2.51), (3.15), (3.17), (3.20), (3.21), (B.4) and (B.5) one can get

$$M\dot{s}_{\mathrm{r}} + k_{\mathrm{pf}} s_{\mathrm{r}} = k_{\mathrm{py}} r + \Delta x_{\mathrm{f}} + y_{\mathrm{a}}, \tag{B.10}$$

where it is defined

$$y_{\mathrm{a}} = p_{\mathrm{b1}} - M\ddot{y}_{\mathrm{r}} - F_{\mathrm{V}}\dot{y}_{\mathrm{r}}, \tag{B.11}$$

and $k_{\mathrm{pf}} \triangleq F_{\mathrm{V}} + k_{\mathrm{py}}$. Also the fact that $s_{\mathrm{o}} = \dot{y}_{\mathrm{o}} - \dot{y}_{\mathrm{r}} = s_{\mathrm{r}} - r$ has been taken into account. To compute $\dot{x}_{\mathrm{f}}$ equations (3.23) and (3.26) are used to get

$$\begin{aligned} \dot{s}_{\mathrm{f}} &= \bar{\gamma} C(-k_{\mathrm{pf}} s_{\mathrm{f}}) + y_{\mathrm{b}} & \text{(B.12)} \\ y_{\mathrm{b}} &= \bar{p}_{\mathrm{b2}} + b(t)\Delta\dot{y} - \dot{x}_{\mathrm{fd}} + k_{\gamma \mathrm{f}}\dot{\sigma}_{\mathrm{f}}. & \text{(B.13)} \end{aligned}$$

The state r is associated to the observation error. By combining equations (3.10), (3.16) and (B.5) one gets

$$\begin{aligned} r &= \dot{y} - \dot{\hat{y}} + \lambda_{\mathrm{z}} z & \text{(B.14)} \\ &= \Delta\dot{y} + \lambda_{\mathrm{y}}\bar{y} - s_{\mathrm{d}} - k_{\mathrm{d}}\left(\lambda_{\mathrm{z}}\int_0^t z(\vartheta)\mathrm{d}\vartheta + z\right). \end{aligned}$$

Finally, by computing the derivative of (B.14) we get

$$\dot{r} + k_{\mathrm{d}} r = \Delta\ddot{y} + \lambda_{\mathrm{y}}\dot{\bar{y}} + k s_{\mathrm{d}}. \tag{B.15}$$

Thus, the closed loop dynamics is given by (B.10), (B.12) and (B.15).

e) In items b) and c) it is analyzed the case when the state $\boldsymbol{\omega}$ and its derivative $\dot{\boldsymbol{\omega}}$ are bounded and it is shown that all tracking and observation errors tend to zero after Theorem 1. In fact, it can be shown that if only the state $\boldsymbol{\omega}$ is bounded, then any other signal related to system (B.10), (B.12) and (B.15) is bounded as well (*e. g.* y, $\dot{y}$, $\ddot{y}$, Δy, $\Delta\dot{y}$, $\Delta\ddot{y}$, s_{o}, $\dot{s}_{\mathrm{o}}$, etc.). See Arteaga-Pérez *et al.* (2006) for details.

f) As pointed out in Arteaga-Pérez *et al.* (2006), by using Theorem 4.18 in Khalil (2002) the boundedness of $\boldsymbol{\omega}$ can be locally proven by defining a suitable region around the origin

$$\mathbb{D} = \left\{\boldsymbol{\omega} \in \mathbb{R}^3 : \|\boldsymbol{\omega}\| \leq \omega_{\max}\right\}, \tag{B.16}$$

where a function $V(t, \boldsymbol{\omega})$ satisfying $\alpha_1(\|\boldsymbol{\omega}\|) \leq V(t, \boldsymbol{\omega}) \leq \alpha_2(\|\boldsymbol{\omega}\|)$ and

$$\frac{\partial V}{\partial t} + \frac{\partial V}{\partial \boldsymbol{\omega}}\boldsymbol{f}(t, \boldsymbol{\omega}) \leq -W_3(\boldsymbol{\omega}), \qquad \forall\ \|\boldsymbol{\omega}\| \geq \mu > 0, \tag{B.17}$$

can be found. $\alpha_1(\cdot)$ and $\alpha_2(\cdot)$ are class $\mathcal{K}$ functions, $W_3(\cdot)$ is a continuous positive definite function, and $\dot{\boldsymbol{\omega}} = \boldsymbol{f}(t, \boldsymbol{\omega})$. By taking $r > 0$ such that $\mathbb{B}_\mathrm{r} = \{\boldsymbol{\omega} \in \mathbb{R}^n | \|\boldsymbol{\omega}\| \leq r\} \subset \mathbb{D}$ and supposing that $\mu < \alpha_2^{-1}(\alpha_1(r))$, then if the initial condition satisfies $\|\boldsymbol{\omega}(t_0)\| \leq \alpha_2^{-1}(\alpha_1(r))$, $\boldsymbol{\omega}$ will be bounded for all time. Note that, in other words, we just have to find a positive definite function $V(t, \boldsymbol{\omega})$ whose derivative is negative for values of $\boldsymbol{\omega}$ larger than a positive value μ in a region $\mathbb{D}$. We propose

$$V(\boldsymbol{\omega}) = \frac{1}{2} M s_\mathrm{r}^2 + \frac{1}{2} s_\mathrm{f}^2 + \frac{1}{2} r^2. \tag{B.18}$$

The derivative of $V(\boldsymbol{\omega})$ along (B.10), (B.12) and (B.15) can be computed as

$$\begin{aligned} \dot{V}(\boldsymbol{\omega}) = & -k_\mathrm{pf} s_\mathrm{r}^2 + k_\mathrm{py} r s_\mathrm{r} + \Delta x_\mathrm{f} s_\mathrm{r} + y_\mathrm{a} s_\mathrm{r} \\ & + s_\mathrm{f} \bar{\gamma} C(-k_\mathrm{pf} s_\mathrm{f}) + y_\mathrm{b} s_\mathrm{f} \\ & - k_\mathrm{d} r^2 + r(\Delta \ddot{y} + \lambda_\mathrm{y} \dot{\tilde{y}} + k s_\mathrm{d}). \end{aligned} \tag{B.19}$$

Recall that the analysis is only local, so that in the region $\mathbb{D}$ the following bounds can be defined as

$$c_1 = \max_{\forall \boldsymbol{\omega} \in \mathbb{D}} |\Delta x_\mathrm{f} + y_\mathrm{a}| \tag{B.20}$$

$$c_2 = \max_{\forall \boldsymbol{\omega} \in \mathbb{D}} |y_\mathrm{b}| \tag{B.21}$$

$$c_3 = \max_{\forall \boldsymbol{\omega} \in \mathbb{D}} |\Delta \ddot{y} + \lambda_\mathrm{y} \dot{\tilde{y}} + k s_\mathrm{d}| \tag{B.22}$$

$$c_4 = \max_{\forall \boldsymbol{\omega} \in \mathbb{D}} |\bar{\gamma}| \tag{B.23}$$

to get

$$\begin{aligned} \dot{V}(\boldsymbol{\omega}) \leq & -k_\mathrm{py} s_\mathrm{r}^2 + k_\mathrm{py} r s_\mathrm{r} - k_\mathrm{d} r^2 + c_1 |s_\mathrm{r}| \\ & + c_4 s_\mathrm{f} C(-k_\mathrm{pf} s_\mathrm{f}) + c_2 |s_\mathrm{f}| + c_3 |r| \\ \leq & -k_\mathrm{py} s_\mathrm{r}^2 + k_\mathrm{py} r s_\mathrm{r} - k_\mathrm{d} r^2 + c_4 s_\mathrm{f} C(-k_\mathrm{pf} s_\mathrm{f}) + \delta\mu ||\boldsymbol{\omega}||, \end{aligned} \tag{B.24}$$

where it is used $k_\mathrm{pf} = F_\mathrm{V} + k_\mathrm{py}$ and $\delta\mu \triangleq c_1 + c_2 + c_3$. δ and μ are positive constants and μ is small enough. By taking into account (2.44) we obtain

$$\dot{V} \leq -k_\mathrm{py} s_\mathrm{r}^2 + k_\mathrm{py} r s_\mathrm{r} - k_\mathrm{d} r^2 - c_4 k_\mathrm{pf} k_\mathrm{u} s_\mathrm{f}^2 + \delta\mu \|\boldsymbol{\omega}\|. \tag{B.25}$$

If the control gains satisfy

$$k_\mathrm{py} \geq 1 + 2\delta \tag{B.26}$$

$$k_\mathrm{d} \geq \frac{k_\mathrm{py}^2}{4} + 2\delta \tag{B.27}$$

$$k_\mathrm{pf} \geq \frac{2\delta}{c_4 k_\mathrm{u}} \tag{B.28}$$

then it is

$$\begin{aligned} \dot{V} &\leq -\left(s_{\mathrm{r}} - \frac{k_{\mathrm{py}}}{2} r\right)^2 - 2\delta\|\boldsymbol{\omega}\|^2 + \delta\mu\|\boldsymbol{\omega}\| \\ &\leq -\delta\|\boldsymbol{\omega}\|^2 - \delta\|\boldsymbol{\omega}\|(\|\boldsymbol{\omega}\| - \mu). \end{aligned} \tag{B.29}$$

If $\|\boldsymbol{\omega}\| \geq \mu$ then

$$\dot{V} \leq -\delta\|\boldsymbol{\omega}\|^2 \stackrel{\triangle}{=} -W_3(\boldsymbol{\omega}). \tag{B.30}$$

Since for $V(\boldsymbol{\omega})$ one has
$\alpha_1(\|\boldsymbol{\omega}\|) \stackrel{\triangle}{=} \frac{1}{2}\min\{M,1\}\|\boldsymbol{\omega}\|^2 \leq V(\omega) \leq \frac{1}{2}\max\{M,1\}\|\boldsymbol{\omega}\|^2 \stackrel{\triangle}{=} \alpha_2(\|\boldsymbol{\omega}\|)$ and $W_3(\boldsymbol{\omega})$ is a continuous positive definite function, the conditions imposed in Theorem 4.18 in Khalil (2002) are fulfilled and the boundedness of the state $\boldsymbol{\omega}$ is guaranteed. Note that according the discussion of items b) and c) this implies the convergence to zero of all tracking and observation errors.

△

Remark 5
The discussion of this appendix shows that tracking and observation error theoretically do tend to zero. From a practical point of view, however, guaranteeing the boundedness of x_{f} in (2.46) does NOT guarantee a priori the boundedness of the pressures $p_1 = x_3$ and $p_2 = x_4$. However, this is given by item 1. of Remark 2. This implies that the limit cases are four: $(x_3 = \mathrm{p_s}, x_4 = \mathrm{p_s})$, $(x_3 = p_{\mathrm{atm}}, x_4 = \mathrm{p_s})$, $(x_3 = \mathrm{p_s}, x_4 = p_{\mathrm{atm}})$ and $(x_3 = p_{\mathrm{atm}}, x_4 = p_{\mathrm{atm}})$. Since $A_2 > A_1$, the maximal value that physically x_{f} can reach is bounded by $|x_{\mathrm{f}}| \leq A_2(\mathrm{p_s} - p_{\mathrm{atm}})$. Thus, care should be taken so that

$$|x_{\mathrm{fd}}| < A_2(\mathrm{p_s} - p_{\mathrm{atm}}) \tag{B.31}$$

is satisfied. △

Bibliography

Deutsches Institut für Normung e. V. (1984),'Dichte; Begriffe, Angaben', *DIN 1306*, Deutsches Institut für Normung e. V.,

Deutsches Institut für Normung e. V. (1990), 'Referenzzustand, Normzustand, Normvolumen; Begriffe, Werte', *DIN 1343*, Deutsches Institut für Normung e. V.

Deutsches Institut für Normung e. V. (1989), 'Pneumatic fluid power – Components using compressible fluids – Determination of flow rate characteristics', *ISO 6358*, ISO (International Organization for Standardization)

Arteaga–Pérez, M.A., Castillo–Sánchez, A.M., and Parra–Vega, V. (2006), 'Cartesian Control of Robots without Dynamic Model and Observer Design', *Automatica*, 42, 473–480.

Arteaga-Pérez, M.A., and Kelly, R. (2004), 'Robot Control without Velocity Measurements: New Theory and Experimental Results', *IEEE Transactions on Robotics and Automation*, 20, 297–308.

Beater, P. (2007), *Pneumatic Drives*, Springer-Verlag Berlin Heidelberg.

Bigras, P. and Khayati, K.(2002), 'Nonlinear observer for pneumatic system with non negligible connection port restriction', in *Proceedings of the American Control Conference, Anchorage, Alaska*, May, 3191–3195.

Böge, A. (1999), *Das Techniker Handbuch: Grundlagen und Anwedungen der Maschinenbau-Technik*, Friedrich Vieweg und Sohn Verlagsgesellschaft mbH, Braunschweig/Wiesbaden.

Göttert, M., and Neumann, R. (1999), 'Nichtlineare Regelungskonzepte fuer servopneumatische Roboter', in *Proceedings 3. Deutsch–Polnisches Seminar Inovation und Fortschritt in der Fluidtechnik, Zakopane, Poland*, September.

Göttert, M., and Neumann, R. (2007), 'Bahnregelung servopneumatischer Antriebe - ein Vergleich von linearen und nichtlinearen Reglern', *Automatisierungs Technik*, 55(2), 69–74.

Guenther, R., Perondi, E.A., DePieri, E.R., and Valdiero, A.C. (2006), 'Cascade controlled pneumatic positioning system with LuGre model based friction compensation', *Journal of the Brazilien Society of Mechanic Science and Engineering*, 28, 48–57.

Gulati, N. and Barth, E.(2005), 'Non-linear pressure observer design for pneumatic actuators', in *Proceedings of the 2005 IEEE/ASME International Conference on Advanced Intelligent Mechatronics, Monterrey, California*, July, 783–788.

Hermann, R., and Kerner, A. (1977), 'Nonlinear Controllability and Observability', *IEEE Transactions on Automatic Control*, AC-22, 728–740.

Ioannou, P.A., and Sun, J. (1996), *Robust Adaptive Control*, U. S. A.: Prentice Hall.

Kagawa, T. y Tokashiki, L. y Fujita, T. (2002), 'Influence of aire temperature change on equilibrium velocity of pneumatic cylinders', *Journal of Dynamic Systems, Measurement and Control*, June, 124, 336–34.

Khalil, H.K. (2002), *Nonlinear Systems, 3rd ed*, Prentice Hall.

Kothapalli, G., and Hassan, Y.M. (2007), 'Design of a Neural Network Based Intelligent PI controller for a Pneumatic System', *IAENG International Journal of Computer Science*, 35, 69–74.

Ning, S., and Bone, G.M. (2002), 'High steady-state accuracy pneumatic servo positioning system with PVA/PV control and friction compensation', in *Proceedings of the IEEE International Conference on Robotics and Automation, Washington, DC*, May, 2824–2829.

Ning, S., and Bone, G.M. (2005), 'Experimental comparison of two pneumatic servo position control algorithms', in *Proceedings of the IEEE International Conference on Mechatronics and Automation, Niagara Falls, Canada*, July, 37–42.

Pandian, S. y Takemura, F. y Hayakawa, Y. (2002), 'Pressure observer-controller design for pneumatic cylinder actuators', in *IEEE Transactions on Mechatronics*, 7, December, 490–499.

Perondi, E.A. (2002), *Controle Não-Linear em Cascata de um Servoposicionador Pneumático com Compensação de Atrito*, Tese de Doutorado, Departamento de Engenharia Mecânica, Universidade Federal de Santa Catarina, Brasil.

Richer, E., and Hurmuzlu, Y. (2000), 'A high performance pneumatic force actuator system: Part II - Nonlinear controller design', *Transactions of the ASME*, 122, 426–434.

Sawodny, O., and Hildebrandt, A. (2002), 'Aspects of the control of differential pneumatic cylinders', in *10th German Japanese Seminar on Problems in Dynamical Systems, Kanazawa*, June.

Shen, X., Zhang, J., Barth, E.J., and Goldfarb, M. (2006), 'Nonlinear model-based control of pulse width modulated pneumatic servo systems', *Journal of Dynamic Systems, Measurement and Control, Transactions of the ASME*, 128, 663–669.

Sobczyk, M.R., and Perondi, E.A. (2006), 'Variable structure cascade control of a pneumatic positioning system', *ABCM Symposium Series in Mechatronics*, 2, 27–34.

Weist, J., and Arteaga–Pérez, M.A. (2009), 'Comparison of different control algorithms for pneumatic actuators', in *Proceedings CD-ROM Congreso Anual de la Asociacin de México de Control Automático (AMCA). Zacatecas, México*, 30th September to 2th October.

Weist, J., Arteaga–Pérez, M.A., de la Cruz, L., and Hebisch, H. (2011), 'Model free control for differential pneumatic pistons: experimental comparison', *International Journal of Control*, 84-1, 138–164.

Wu, J., Goldfarb, M. and Barth, E. (2003), 'The role of pressure sensores in the servo control of pneumatic actuators', in *Proceedings of the American Control Conference, Denver, Colorado, United States of America*, June, 1710-1714.

Zeitz, M. (1984), 'Observability canonical (phase-variable) form for nonlinear time-variable systems', *International Journal of Systems Science*, 15, 949–958.

Zhu, Y. (2006), *Control of pneumatic systems for free space and interaction tasks with system and environmental uncertainties*, Dissertation, School of Vanderbilt University, Nashville, Tennessee, United States of America.